UNIVERSITÀ
DEGLI STUDI
DI PADOVA

Università degli Studi di Padova

Dipartimento di Ingegneria Industriale

SCUOLA DI DOTTORATO DI RICERCA IN INGEGNERIA INDUSTRIALE
INDIRIZZO INGEGNERIA CHIMICA, DEI MATERIALI E MECCANICA
CICLO XXVIII

Technologies to study the mechanosensitive response of cardiovascular cell cultures

Direttore della Scuola : Ch.mo Prof. Paolo Colombo
Coordinatore d'indirizzo: Ch.mo Prof. Enrico Savio
Supervisore :Ch.mo Prof. Nicola Elvassore
Co-Supervisore: Ch.mo Prof Juan Carlos Izpisua Belmonte

Dottoranda: Lia Prevedello

Foreword

The work presented in this thesis was carried out at the Dipartimento di Ingegneria Industriale-sede M of the Università degli Studi di Padova and at the Venetian Institute of Molecular Medicine of the Fondazione per la Ricerca Biomedica Avanzata in Padova under the supervision of Prof. Nicola Elvassore

Part of the PhD project was performed at the Salk Institute for Biological Studies in La Jolla, Californa, USA at the Gene Expression Laboratory under the supervision of Prof. Juan Carlos Izpisua Belmonte.

All the material reported in this dissertation is original unless explicit references to studies carried out by other people are indicated.

During the PhD program the following publication has been published

> Giulitti S, Magrofuoco E, Prevedello L, Elvassore N (2013). Optimal periodic perfusion strategy for robust long-term microfluidic cell culture. LAB ON A CHIP, vol. 13, p. 4430-4441, ISSN: 1473-0197, doi: 10.1039/c3lc50643f

The following posters has been presented

> Prevedello L., F. Michielin ,M. Balcon, E. Savio,P. Pavan and N. Elvassore, Microfluidic platform for planar biomechano-stimulations allowing real time imaging of stretched cells. 4th International Conference on Stem Cell Engineering, San Diego (CA) USA, 16-19/03/2014

Sommario

La possibilità di riprogrammare le cellule adulte in cellule pluripotenti indotte, scoperta nel 2006 da Yamanaka, ha aperto nuove allettanti prospettive sia per lo studio dei processi di differenziamento che portano allo sviluppo di organi e tessuti, sia per lo sviluppo di nuovi approcci terapeutici. Per poter sfruttare a pieno le potenzialità nel campo della ricerca scientifica e medica delle cellule staminali indotte, è tuttavia necessario sviluppare tecnologie innovative che permettano di ricreare *in vitro* le caratteristiche riscontrate *in vivo*. In particolare nell'ultimo decennio è stato scoperto che il microambiente meccanico esercita una notevole influenza sui processi cellulari, regolando la morfologia, l'espressione genica e il differenziamento delle cellule stesse. Nonostante la meccanotrasduzione, ovvero il processo secondo cui gli stimoli meccanici esterni vengono tradotti dalle cellule in processi biologici, sia presente in tutte le cellule, si ritiene che possa avere particolare rilevanza nei tessuti che *in vivo* sono sottoposti a maggiori stimoli meccanici. In particolare, si è visto come gli stimoli meccanici esercitino una notevole influenza nello sviluppo e maturazione dei tessuti del sistema cardiovascolare e come stress meccanici anomali possano essere correlati all'insorgenza di patologie cardiovascolari. Il sistema cardiovascolare riveste un particolare interesse nel mondo scientifico e clinico in quanto le malattie cardiovascolari sono la principale causa di morte al mondo, e anche i costi associati alla prevenzione e al trattamento di tali patologie sono particolarmente rilevanti. Per giunta, la cardio-tossicità è la principale causa di rigetto dei nuovi farmaci, rendendo lo studio del sistema cardiocircolatorio estremamente rilevante anche nella fase di sviluppo farmaceutico.

Lo scopo di questo lavoro è sviluppare nuove tecnologie atte a riprodurre *in vitro* il microambiente meccanico presente *in vivo*, con particolare riferimento al sistema cardiovascolare, per consentire lo studio della risposta cellulare agli stimoli meccanici. Nello specifico, le tecnologie sviluppate potranno essere usate per riprodurre gli stimoli a cui il sistema cardiovascolare è sottoposto durante sforzi intensi, come ad esempio la guida

agonistica di motocicli. In particolare è stato posta l'attenzione alla riproduzione della morfologia delle cellule del tessuto cardiaco e delle deformazioni meccaniche tipiche del sistema cardiovascolare.

In primo luogo, per riprodurre la polarizzazione tipica delle cellule del muscolo cardiaco, sono state delineate o ottimizzate strategie per ottenere colture allineate di cardiomiociti su vetro. L'allineamento viene ottenuto creando linee di esclusione cellulare costituite da un gel di poliacrilamide, alternate a linee in cui l'adesione cellulare viene favorita mediante trattamento con proteine della matrice extracellulare. Lo sviluppo di un metodo robusto e preciso per la realizzazione di colture di cardiomiociti allineati permetterà lo studio dell'effetto della topologia e polarizzazione sull'espressione genica delle cellule, e inoltre permetterà di analizzare la morfologia delle giunzioni cardiache e la trasmissione degli impulsi elettrici tra cellule adiacenti. Successivamente le tecniche di allineamento sono state trasferite anche ai materiali materiali elastomerici, come il PDMS, per permettere la sollecitazione meccanica di colture allineate, similmente a quanto avviene negli organi.

Il primo sistema di stretch meccanico è stato sviluppato per effettuare analisi di estrazione di proteine, RNA o DNA. È costituito da una camera di coltura di 9cm^2 e la stimolazione avviene attraverso la trazione meccanica esercitata da ElectroForce® planar biaxial TestBench (Bose), in questo caso l'allineamento cellulare viene imposto tramite la realizzazione sulla superficie di coltura di canali a differente altezza su cui si dispongono le cellule.

Il secondo sistema di stretch è stato sviluppato principalmente per effettuare analisi di imaging, come immuofluorescenze, e di patch clamp. La camera di coltura è pari a 1cm^2 e la stimolazione meccanica avviene gonfiando una membrana in apposite aree rettangolari di deformazione, che costituiscono circa il 40% della totale area di coltura. In questo caso l'allineamento cellulare viene imposto tramite la realizzazione di righe cellule-repellenti in poliacrilamide, sfruttando lo stesso principio adottato nel caso del vetro.

Entrambi i sistemi di coltura sono stati testati per dimostrarne le biocompatibilità e per verificare che gli stimoli meccanici che sviluppati sono tali da innescare una risposta cellulare.

Summary

The ability to obtain induced pluripotent stem cells starting from adult differentiated cells, discovered in 2006 by Yamanaka, opened new fascinating opportunities for the study of the development of tissues and organs and for the establishment of new therapeutic approaches. To fully take advantage of pluripotent stem cells potentiality for scientific and clinical research, it's necessary to develop also new technologies that will enable the reproduction *in vitro* of the *in vivo* environment.

In the last decade, it was discovered that the mechanical microenvironment has a very marked impact on virtually all cellular processes, ranging fro morphology to gene expression and faith specification. Mechanotransduction, which is the biological process that enable cells to sense and respond to mechanical *stimuli*, is present in all cells, however it is believed that it may have greater influence in tissues that are subjected to higher mechanical *stimuli in vivo*, as in the case of the cardiovascular system. As an example, it has been shown that mechanical cues strongly affect the development and maturation of cardiovascular tissues, and that abnormal mechanotransduction can be linked to the onset of several cardiovascular diseases. There is a great interest in the scientific and clinical research communities on the study of the cardiovascular system since cardiovascular diseases are the principal cause of death worldwide and also the associated health care costs to prevent and treat these pathologies are quite elevated. Moreover, cardiovascular toxicity is the primary cause of drug withdrawal, so the development of novel, more accurate models of the cardiovascular system are extremely important also for pharmaceutical research and development.

The aim of this work is to develop innovative technologies to reproduce *in vitro* the *in vivo* mechanical microenvironment, specifically that of the cardiovascular system, to gather further knowledge on the biological response to mechanical cues. In particular, these newly developed technologies could be used to reproduce the mechanical *stimuli* exerted on the cardiovascular system by physical strain, such as agonistic motorcycle driving.

Specifically, in this thesis the focus was on reproducing the characteristic morphology of cardiovascular tissues' cells and on mimicking mechanical strains typical of the cardiovascular system. Firstly, the polarization typical of cardiac muscle cells has been reproduced on glass, outilining and optimizing strategies to obtain aligned cardiomyocytes. The alignment is imposed creating a linear pattern of cell repulsive stripes, made of polyacrylamide hydrogels, alternated with protein-coated cell adhesive stripes. The establishment of a robust and precise glass patterning technique during this work will allow to study in depth the effect of topology and polarization on cellular gene expression and also will enable the study of cardiomyocytes intercalated discs' morphology and the transmission of electrical signals among neighboring cells.

Later on, the patterning techniques were transferred to elastomeric materials, such as PDMS, to perform mechanical stimulation of aligned cardiomyocytes cultures, reenacting the organ and tissues environment.

The first stretching device realized was designed to perform biological assays that require an elevated quantity of starting material, such as protein, DNA or RNA extractions. For this reason the culturing area is $9cm^2$, and mechanical deformation is imposed through the mechanical traction generated by the ElectroForce® planar biaxial TestBench (Bose). In this device, cell alignment is obtained through physical pattering, which means the creation of PDMS channels of different heights along which the cells are seeded.

The second stretching device realized during this work was designed mainly for imaging analysis, such as immunofluorescence, and patch clamp. The culturing area is $1cm^2$, and mechanical deformation is generated inflating a PDMS membrane in specifically designed rectangular areas that constitute about 40% of the total culturing area. In this case, cell alignment is performed realizing cell repellent polyacrylamide stripes, harnessing the same scientific principle used for glass patterning.

Both culturing device were tested to verify their biocompatibility and ensure that the mechanical *stimuli* they can impose are sufficient to trigger a biological response.

Index

Chapter one
Introduction

The ability to reprogram adult differentiated cells into pluripotent stem cells, named induced pluripotent stem cells (iPSC), firstly discovered by Yamanaka in 2006 in mouse and in 2007 for humans (Takahashi and Yamanaka 2006, Takahashi *et al.* 2007) brought the promise of opening fascinating new opportunities in the study of the development of tissues and organs, in diseases modeling, in drug testing and in the development of novel personalized therapies (Nishikawa *et al.* 2008, Dash *et al.* 2015), by allowing to produce large amounts of terminally differentiated cells that were other ways unfeasible to obtain.

As the scientific research strives to render ever more efficient cellular reprogramming, reducing both time and costs associated and widening the possible application of this biological breakthrough, the necessity to develop new technologies to take full advantage of the iPSC potential also arises. These new technologies will have to reproduce the *in vivo* environment, both to help understand the process of differentiation, tissue development and damage repair at the biological level and to obtain differentiated and mature cells for drug testing and therapeutic approaches (Shao *et al* 2015).

The work of this doctoral thesis was focused on the development of new technologies specifically addressed to study the cardiovascular system, but that could be applied also in other case studies.

In the introductory chapter cellular mechanotransduction and the cardiovascular system will be described, focusing on the physiology of the latter two main components to elucidate the features that biological *in vitro* models need to reproduce. Then, the interplay between the onset of cardiovascular diseases and pathological mechanotransduction will be elucidated, moreover also the study of the physiological response to mechanical *stimuli* derived by demanding physical activity will be discussed, focusing on the effect of agonistic motorbike driving. Finally, the aim of the doctoral studies and the work organization will be defined.

1. Cellular mechanotransduction

Mechanotransduction describes the cellular process by which the mechanical properties of the extracellular environment, such as substrate stiffness, mechanical forces, cell morphology and shear stress (figure 1.1.1), are sensed and translated into biochemical signals that induce an adaptive intracellular response (Nakayama *et al* 2014).

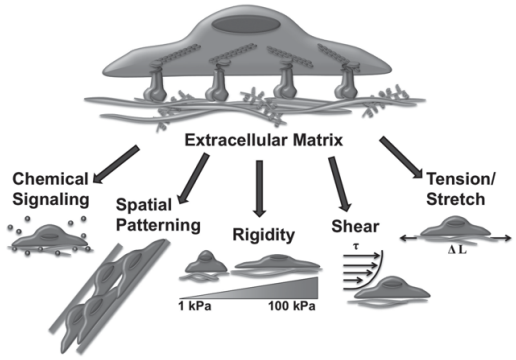

Figure 1.1.1 *Graphic summary of the mechanical properties of the extracellular environment that elicit an adaptive intracellular response (curtesy of Nakayama et al. 2014).*

Though mechanotransduction was known since many years, the impact of extracellular mechanical cues in virtually all cellular process has been demonstrated recently, ranging from proliferation and protein expression to cell faith specification and organogenesis (Brown and Discher 2009, Mammoto *et al.* 2012, Stewart *et al* 2011).

The ability of cells to properly address changes in their microenvironment is paramount for the development and maintenance of organs and tissues exposed to varying mechanical stress, and also, more broadly, in the tuning of physiological processes which affect the organism as a whole (Jaalouk and Lammerding 2009).

2. The cardiovascular system

The cardiovascular system is an organ system devoted to the transport of blood in the body, along with all the necessary compounds dissolved in it, such as oxygen, nutrients and hormones just to name a few.

As the name states, the cardiovascular system is composed by the heart, which pumps oxygenated blood, and the vascular system.

2.1.The human heart

The human heart is a four chambered organ composed of two atria and two ventricles (figure 1.2.1), with the right side receiving deoxygenated blood from the body at low pressure and pumping it to the lungs (pulmonary circulation) and the left side receiving oxygenated blood from the lungs and pumping it at high pressure around the body (systemic circulation).

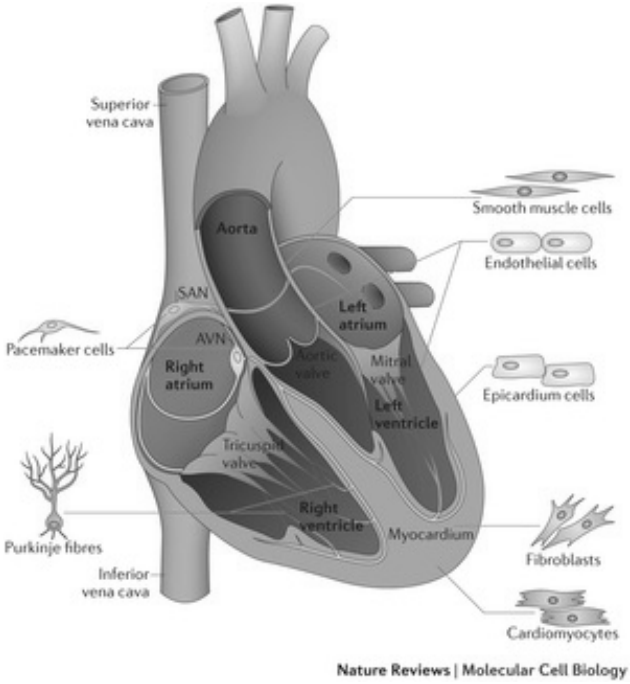

Figure 1.2.1 *Representation of the heart and of the cell types that define its structural, biochemical, mechanical and electrical properties (curtesy of Xin et al. 2013).*

The heart is composed by several cell types, summarized in figure 1.1.1, all necessary to determine the physiological structural, biochemical, mechanical and electrical properties. More than 50% of cells comprised in the heart are cardiac fibroblast originated from the epicardium. The endocardium is composed by endothelial cells, which also form the interior lining of blood vessels and cardiac valves. Finally, the myocardium, the actual muscular wall of the heart, is composed by cardiomyocytes that are distinguished in atrial

and ventricular subtypes and also give rise to specialized cells that generate and conduct electrical impulse, called pacemaker cells and Purkinje fibers.

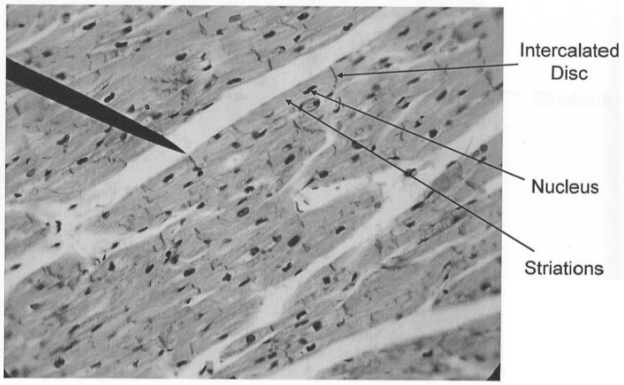

Figure 1.2.2 *Longitudinal section of cardiac muscle fibers (adapted from anatomyphysiologyibis240.blogspot.it)*

Cardiomyocytes are arranged in interlacing bundles to form the heart muscle, *in* vivo they are highly polarized and show a characteristic rectangular shape roughly 20µm wide and 100µm long, as represented in figure 1.2.2. The intercalated disks, highlighted in the picture, are a prominent and unique feature of cardiomyocytes that constitute the electromechanical coupling of the cells and allow the electrical signal propagation in the heart muscle.

2.2.The circulatory system

The circulatory, or vascular, system is primarily divided in arteries, that disturbed the oxygen-rich blood from the heart to the body, and veins, which carry the blood back to the heart; it is so vast and articulated that if all the blood vessel in a human body were lined up, they would stretch for almost 100'000Km. Vessels are classified based on size, starting from arteries and veins, down to arterioles and venules and finally capillaries, that actually distributed the blood to the different tissues and cells (figure 1.2.3).

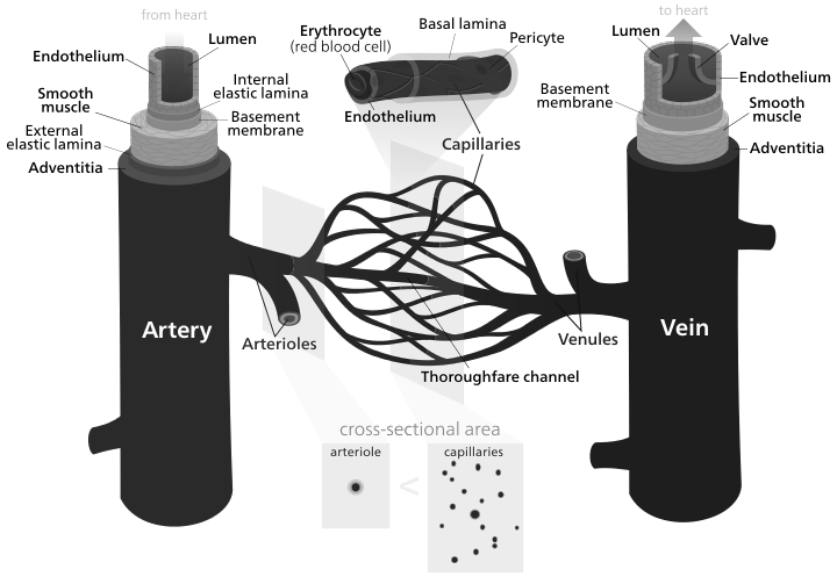

Figure 1.2.3 *Schematic representation of the circulatory system: the main vessels are arteries and veins, which respectively take the blood from and to the hear, and are composed of different layers. The vessels then reduce in size down to arterioles and venules and finally to capillary, which actually deliver blood at the tissues and cellular levels. (picture from Wikipedia).*

The blood vessels, except capillaries, are composed of three different layers: the innermost is the tunica intima, which is composed of endothelial cells and forms a continuum with the heart endocardium; the intermediate level is called tunica media, and is composed of circularly arranged smooth muscle cells and elastin, it is generally the bulkiest layer of the vessel and it maintains blood pressure and proper circulation; finally the outer layer is the tunica adventitia, mainly made by collagen fibers, that serves to protect and reinforce the vessel and connect it to the surroundings.

2.3.Socio-economic relevance of the cardiovascular system

There is a great scientific and medical interest in the study of the cardiovascular system since cardiovascular diseases are the leading cause of death worldwide (figure 1.2.4a). According to the World Health Organization in 2012 about 30% of all deaths, which equals 17.5 million deceases, were due to cardiovascular diseases (CVDs) and the trend has been growing in the last years.

The relevance of these diseases is higher in the developed countries (for instance it accounts for 42% of deaths in Europe), mainly because of the advancing age and the minor mortality associated with infectious diseases. Moreover, thanks to progress in patient care, the mortality rate of CVDs has been reduced, but usually at the cost of increasing morbidity and chronic pathological conditions, as an example, in the USA alone, 26.6 million people are diagnosed with heart diseases, which equals 11.3% of the adult population.

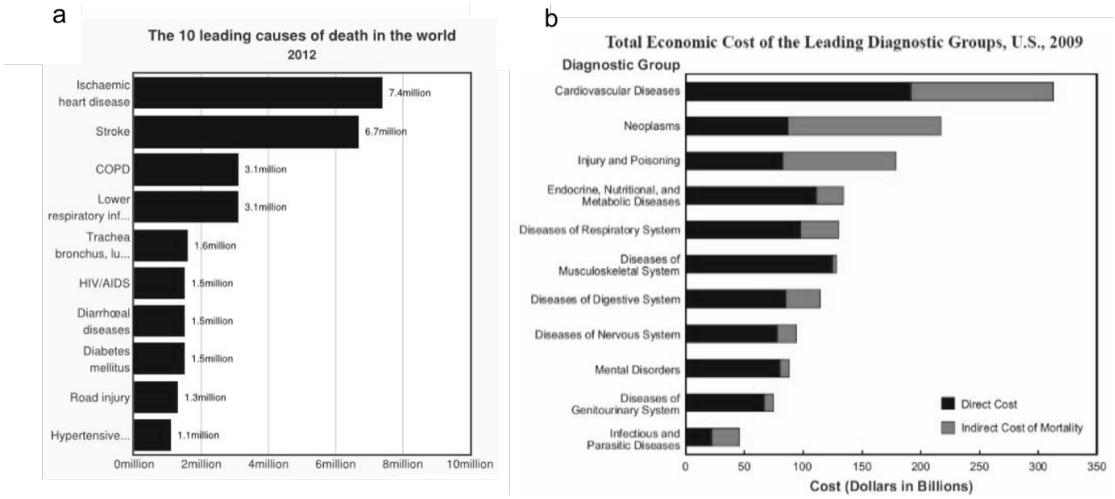

Figure 1.2.4 *Statistics representing the relevance of cardiovascular diseases on global health (figure 1.1.4a, WHO 2012) and on economy, as shown by US health care costs (NIH Fact Book 2012).*

Accordingly, also the associated cost for the cure and the prevention of cardiovascular diseases are quite high (figure 1.2.4b). The Centre for Diseases and Control and Prevention estimates the total cost associated to CVDs in the United States to be around 444 billion $ per year, roughly 1$ every 6$ spent in health care, while in Europe, the European Heart Network reposts an economic burden, comprising both direct and indirect costs, of 196 billion € per year.

Moreover, another major focus of scientific research on the cardiovascular system is the development of novel drug screening *in vitro* high-throughput assays to allow an earlier identification of drugs cardiovascular hazard. In fact, nowadays cardiovascular toxicity is

the major cause of drug attrition and withdrawal, and adverse cardiovascular safety pharmacology findings were responsible for more that 33% of safety-related drug withdrawals in the period 1990-2006 (Peters *et al* 2015).

3. Cardiovascular diseases and pathological mechanotransduction

Given the constant mechanical stimulation typical of the cardiovascular system, it is easy to deduce that mechanotransduction plays a pivotal role in this tissue development and maintenance and that abnormalities in mechanical signalling might lead to the disruption of normal tissue function and the onset of diseases.

A pathological mechanotransduction response can be due both to an impairment of the cellular mechanosensitive apparatus, or to a physiological mechanotransduction signalling of abnormal mechanical conditions. While the former is mainly attributable to genetic diseases, the onset of the latter can manifest frequently with age or other ways induced changes in the body physiology.

3.1. Cardiac Hypertrophy

Increased mechanical loads and the resulting morphological changes at the organ (ventricles) and cellular (cardiomyocytes) levels are characteristic of several cardiomyopathies (Gerdes 2002).

For example, in concentric hypertrophy the pressure overload causes thickening of the ventricular chamber due to increased cross-sectional area of the cardiomyocytes through parallel addition of myofibrils (Mc Cain and Parker 2011, Göktepe *et al.* 2010). On the other hand, volume overload triggers eccentric hypertrophy, which at the cellular level consists in the lengthening of cardiomyocytes through the addition, is series, of sarcomeres and at the tissue level the outcome is thinning of the ventricular wall, dilation of the chamber and elevated stress (Mc Cain and Parker 2011, Göktepe *et al.* 2010). In both hypertrophic cardiomyopathies, the pathological mechanical *stimuli*, respectively pressure or volume overload, are the driving force for diseases onset and progression (Kumar *et al.* 2005).

Maladaptive hypertrophy is also associated with myocardial infarction, as the remaining myocytes strive to compensate the mechanical overload resulting from the infarction scarring.

3.2.Arrhythmias

Arrhythmia refers to an abnormal heart rhythm, which means the heart beat is either too fast (tachycardia), too slow (bradycardia) or irregular, if the arrhythmic conditions persist for long period, the heart is no longer able to supply the necessary blood flow to the organism leading to organ damage and in the most severe cases to death.

Despite heart mechanical dysfunction is closely associated to sudden cardiac death caused by arrhythmias, a casual link between pathological mechanical forces and electrical instability hasn't been fingered out yet (Laurita and Rosenbaum 2008).

The existence of a Mechano-electric Feedback, through which electrical excitation of myocytes is converted in mechanical contraction that in turn affects the electrical excitation of cells, probably enforced by the presence of stretch-activated channels, strongly points toward the existence of that casual link (Takahashi *et al* 2013)

3.3.Vascular diseases

In the vascular system, the endothelial cells composing the inner layer of the vessel are subjected to constant shear stress, moreover, in arteries, the pulsing pressure enforced by the beating heart causes also a cyclic stretch of the vessels walls (Tarbell *et al.* 2014).

Shear stress caused by the blood flow plays a major role in determining vascular endothelial cells function and phenotype (Collins and Tzima 2011). It has been shown that high, uniform shear stress has a atheroprotective role, reducing the expression of inflammatory proteins and the recruitment of leukocytes at the vascular wall, whereas, low oscillatory shear stress has an opposite effect. As a result, atherosclerosis development is highly localized around branches and bends of the arteries, where the blood flow is typically disturbed (Gimbrone and García-Cardeña 2013, Bryan *et al.* 2014).

Cyclic mechanical stretch, on the other hand, primarily affects vascular smooth muscle cells, regulating various biological processes such as proliferation, apoptosis and migration and influencing also the synthesis and composition of the exctracellular matrix secreted by the cells. The increased vascular wall stress caused by chronic hypertension has been implicated in the pathogenesis of cardiovascular diseases as the additional strain in vascular smooth muscle cells activates a signalling cascade that leads to cell hyperplasia and hypertrophy and increased deposition of extracellular matrix. On the macroscopic level the hypertension-induced vascular remodelling leads to pathological structural changes in the arterial wall such as increase of wall thickness and reduction of the luminal diameter (Haga *et al.* 2007, Birukov 2009, Yang *et al.* 2014).

4. Effect of cardiovascular stress elicited by agonistic motorcycles driving

Physical activities that require high cardiac stress for a prolonged period may trigger heart remodelling (Mihl *et al.* 2008) thus exposing the subject to a higher risk of developing heart diseases, mainly associable to heart hypertrophy and severe cardiac arrhythmias that may lead, in the worst case scenario, to sudden death, that every year affects 1:200'000 athletes (Furlanello *et al.* 1998).

Therefore, it would be interesting to study the effect of prolonged and abnormally high mechanical strain on the vasculature and identify the biochemical mechanism that leads to the onset of a pathological response. Since this doctoral studies were founded by a scholarship on "Upgrade and expansion of motorcycle industry" (Founds from "Legge 170" from the Italian Minister of Instruction, University and Research), in this context it could be interesting to study the response of the cardiovascular to the mechanical stress caused by motorcycle driving, especially in agonistic competitions.

During motorbikes competition the cardiovascular system is subjected to extremely intense strain, with heart rate that can reach up to 90% of the athlete maximum rate, especially when driving the more powerful motorbike classes such as 250GP and 600cc and increased blood pressure (D'Artibale *et al*. 2008). Moreover, in particular during motocross and endurance

competitions, also the levels of biomarkers associated with oxidative stress and its downstream effects were shown to be higher than the baseline values, indicating a strong biological solicitation (Ascensao *et al.* 2007, Konttinen *et al* 2007).

The evaluation of the effect of agonist motorcycles-driving associated cardio-vascular stress will be a first case study of the effect of the physical strain resulting in general from agonistic physical activity and could bring new insight in the biological relationship between abnormal mechanical stress, cardiovascular remodelling and onset of pathological remodelling.

5. Aim

The aim of this thesis is to develop new technologies to allow the study of the response of the cardiovascular system to external mechanical *stimuli*.

As described before, there is an increasing awareness on the effect of the mechanical microenvironment on cellular behaviour and fate specification. To further improve the scientific knowledge in the role played by mechanical forces in organ development, physiology and pathogenesis, and discover new therapeutics approaches for the prevention and cure of cardiovascular diseases an improvement in biological culturing tools is required.

These novel technologies will have to reproduce the *in vivo* mechanical environment, to recreate both physiological and pathological conditions and allow the study the biological response at the cellular level.

Specifically, in this work the focus was on developing techniques to culture cells on patterned substrates, in order to recreate the highly organized and polarized morphology of the cardiac tissue, and on developing stretching devices to culture cells in mechanically active conditions.

The patterning techniques were developed also for elastomeric substrate, thus allowing the stimulation of align cardiomyocytes, mimicking as faithfully as allowed by current technologies the *in vivo* settings.

In the second chapter the development and optimization of patterning techniques for different materials will be described, presenting the results obtained and giving insight of the

impact and usefulness these technologies will have in defining the future innovative biological research.

In the third chapter the development of devices to culture cells in mechanically active conditions will be addressed, presenting the manufacturing protocols established and the results obtained in the preliminary experiments.

Finally, the achievements of this work will be summarized and the future applications of the newly developed technologies will be discussed.

Chapter two
Patterning Techniques

The pattering techniques established and optimized during this work are aimed at recreating the geometrical order of several human tissues, such as smooth muscle and cardiac muscle, in order to investigate the physiological and pathophysiological response of cultured cells to external *stimuli* in a system that resembles more closely the *in vivo* environment.

During the thesis the main goal was to develop linear pattern to align cultured cells and to be able to control the number of adjoining cells. As a result, the geometries employed were either lines wide 50µm for single cell alignment or wider, or rectangles of 50µm wide and 100µm long for single cardiomyocytes pattern or longer according to the number of adjoining cells desired.

Cell patterning was developed both for glass substrates, to study the structure of the cell to cell junction and the electrophysiology of cardiomyocytes at rest, and for elastomeric substrates such as PDMS, to study the modification in the cellular physical and electrical coupling following mechanical stress.

In this chapter firstly the general principle used to achieve the pattern both on glass and PDMS will briefly described. In the second paragraph two different protocols for glass patterning will be presented and the results obtained confronted. Afterwards the development of patterning techniques for the elastomeric substrates will be described analyzing all the steps that led to the establishment of the optimized protocol. Finally, the overall outcome resulting from patterning on the two different substrates will be considered in the view of further optimization and exploitation.

1. Introduction to cell patterning

The basic idea of cell patterning is to generate cell repulsive or cell attractive areas of defined geometry.

The methods based on the generation of a cell attractive areas relay on the need of a protein or external cellular matrix coating for cellular attachment, thus localizing the coating just in the cell attractive areas allows the creation of the desired pattern. The most widely known methods used in this case is Micro-Contact Printing, µCP, developed by George M. Whiteside's group at Harvard University for the generation of Self Assembled Monolayers of ink on a surface and readapted in cell biology to print proteins (Pearl A. *et al* 2009). In this case a mold presenting the features of the desired pattern is realized in PDMS through standard soft-lithography techniques (figure 2.1.1a), the protein solution is poured on the mold (figure 2.1.1b), the mold is then pressed on the substrate (figure 2.1.1c) transferring the protein pattern to the substrate (figure 2.1.1d).

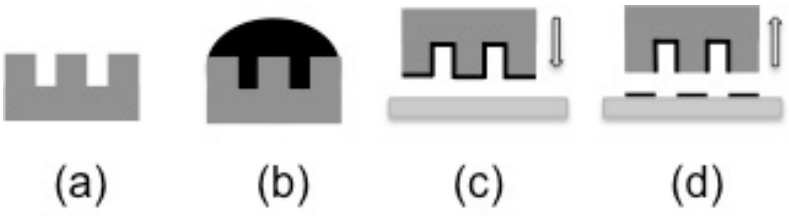

Figure 2.1.1 *µCP steps: a PDMS mold is created (a), the protein solution is poured on the mold (b) the mold is pressed on the substrate (c) and upon removal the protein in transferred in the desired pattern(d).*

µCP has become widely used because of its low costs, high throughput and ease of use. The technique presents also some drawbacks such as mold deformability and protein solution mobility during the transfer that limit the features that can be accomplished and its reliability, moreover the efficiency of PDMS to PDMS transfer is low, since the transferring surface and the accepting surface have the same affinity to the solution.

For these reasons in this work it was preferred to use different patterning techniques relying on the generation of cell repulsive areas constituted by a layer of ultra-soft hydrogel that mechanically inhibits cells attachment to the substrate.

The effect of substrate stiffness on cell morphology and transcriptional activity has been known and investigated for many years following the pioneering studies of Wang and co-workers on the effects of stiffness on cellular behavior. Wang group first reported a destabilized adhesion of fibroblast and epithelial cells cultured on relatively soft substrates, E<20kPa, (Pelham and Wang 1997), then showed a decrease of DNA synthesis and increase of cellular apoptosis in normal cells when cultured on polyacrylamide hydrogels with a Young Modulus of 4.7 kPa compared to stiffer substrates (Wang *et* al 2000).

More recently Marklein and coworkers showed the effect of substrate stiffness on the proliferation of human Mesenchymal Stem Cells, hMSC, as shown in figure 2.1.2. Methacrylated hyaluronic hydrogels (MeHa) were obtained *via* chemical crosslinking, then, where higher stiffness was required, further crosslinking of the remaining unconsumed methacrylated was obtained *via* UV exposure. The two stiffness obtained in this way showed remarkable differences in the growth rates of seeded hMSC, and it was reported that eventually the highly different proliferation rates can lead to the formation of a cellular pattern when highly crosslinked MeHa hydrogels were created alongside softer ones (Marklein *et al* 2010).

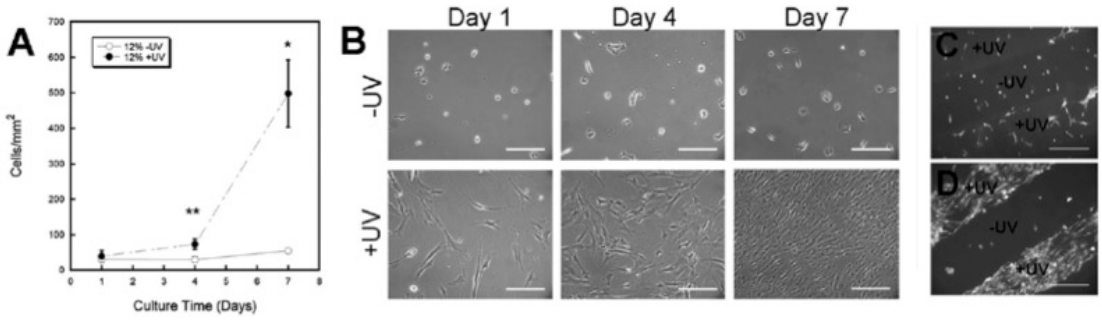

Figure 2.1.2 *Effect of substrate stiffness on hMSC proliferation. A) cell density variation during culturing days, on stiff substrates (+UV) cell number increase following an exponential growth, on soft substrates (-UV) the cellular growth is almost inexistent. B) Images of the cultured hMSC on stiff (+UV) and soft (-UV) substrate at different time points. The different growth rate can be exploited to obtain a patterned culture c) 1 day after seeding and d) 7 days after seeding. (Readapted from Marklein et al 2010).*

In this work poly-acrylamide (PA) hydrogels were used due the wide range of stiffness that can be obtained varying the percentage of the linear acrylamide and of the bis-acrylamide (Tse and Engler 2010) and also because a protocol for the fabrication of PA hydrogel of defined Young Modulus was already established in the laboratory (Aragona *et al* 2013, Dupont *et al* 2011).

Figure 2.1.3 graphically summarizes the working principle of the soft polyacrylamide patterning technique used during this work.

A layer of soft hydrogel is generated on the intended cell repulsive areas whereas the cell attractive areas are left empty (figure 2.1.3a). After substrate coating with an adequate extracellular matrix protein the cells are seeded (figure 2.1.3b). Cells that are on the hydrogel-free areas are able to attach to the substrate, spread and proliferate while the cells on the soft hydrogel are unable to regain a physiological morphology and eventually encounter apoptosis (figure 2.1.3c-d).

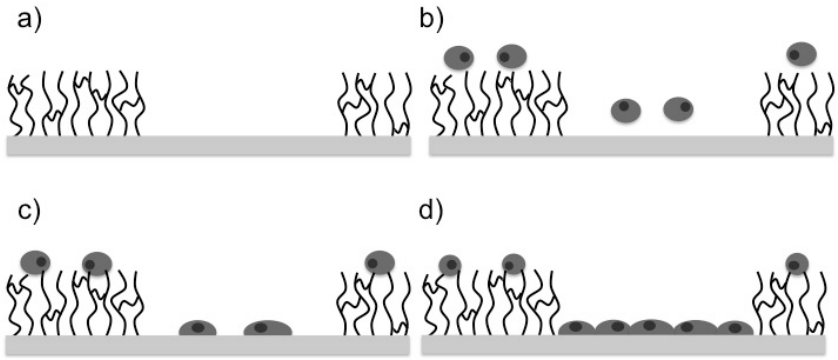

Figure 2.1.3 *Working principle of PA hydrogel. The soft hydrogel is created on a pattern on the surface (a), cells are seeded homogenously (b), only the cells in the hydrogel free areas are able to attach and spread (c), after some day in culture cells on the cell attractive areas replicate and create a uniform layer whereas cells on the hydrogel can't proliferate and undergo apoptosis (d).*

The same mechanism was used for patterning both glass and elastomeric substrates though the optimization of the technique led to the development of two different protocols for the two substrates.

2. Glass Patterning

Pattern on glass was realized mainly to allow the study of the electromechanical coupling of cardiomyocytes in rest conditions, recreating the morphology of the cardiac muscle described during the introductory chapter.

The choice of using a glass surface for these experiments was based on the many different factors among which the optical transparency of glass, the possibility to use confocal microscopy compatible glass slides, the established biological protocols for cell culturing on glass and the ease of fabrication.

Two different techniques can be used to pattern a polyacrylamide hydrogel on a glass surface: photo activated polymerization of acrylamide limited to the cells repulsive areas of the pattern (a.k.a photo-patterning), or chemical activation of acrylamide protecting the cells attractive areas through photolithography. In this work both methods have been employed in order to determine which one provides the the best results in terms of geometrical accuracy and reproducibility.

For these experiments round microscopy glass slides of 25mm diameter (Menzel-Glaser) were employed.

2.1.Photo-patterning

The first technique examined was the photo-activated polymerization of acrylamide since this method, allowing the direct formation of a patterned hydrogel, requires less manufacturing steps and thus is faster.

In this case the acrylamide hydrogel, responsible to hinder cell adhesion, is locally polymerized only in the cell repulsive areas of the pattern exposing the prepolymer solution to UV light through a photomask. The UV light is able to pass through the transparent spaces of the mask, that reproduce the cell repulsive geometry, and, interacting with a photo initiator, catalyzes the polymerization in that areas. In the blackened spots of the mask the UV radiation is shielded and the reaction doesn’t occur giving rise to the cell exclusive pattern.

2.1.1. Glass preparation

In order to promote acrylamide adhesion, it is necessary to functionalize the glass surface. Firstly, the glass slides were thoroughly washed with a piranha solution composed of 75%$_{vol}$ sulfuric acid (98% purity, Sigma-Aldrich) and 25%$_{vol}$ hydrogen peroxide (30%$_{wt}$ concentration, Sigma-Aldrich) heated at 60°C to maximize the reactivity of the solution. Afterwards the glass slides were rinsed with deionized water and dried with a flux of air.

Then the glass slides were subjected to plasma treatment to activate the surface. To this purpose the slides were placed in the Plasma Cleaner (Harrick Plasma), the chamber was sealed and vacuum was applied until a pressure of 3 mbar was reached and, after stabilizing the pressure, the plasma switch was activated. The glass slides were treated for two minutes after the generation of the plasma and then removed from the chamber.

Immediately after the plasma activation of the surface the glass slides were treated with a silanizing solution covering the whole activated surface. The solution was composed of 950 µl of ethanol (98% purity, Carlo Erba), 50 µl of glacial acetic acid (Sigma-Aldrich) and 3µl of (3-aminopropyl)triethossi-silane (Sigma-Aldrich). The glass slides were left in a laminar flux chemical hood until complete evaporation of the solution, then they were rinsed with ethanol, washed twice with deionized water and placed on a heated plate at 115°C until completely dry.

2.1.2. Acrylamide solution

The polyacrylamide hydrogel employed in the photo activated pattern was composed of purely linear acrylamide monomers to minimize the stiffness and maximize the cell repulsive effect. A stock solution of linear acrylamide prepolymer composed of 79% MilliQ water, 20% acrylamide at 40%$_{wt}$ concentration and 1% HEPES 1M buffered to obtain a PH of 8 was realized. This solution can be prepared in advance and conserved

for one month at 4°C. Prior to use the solution was placed in a vacuum chamber at approximately 10^{-2}mbar to strip away dissolved oxygen that may hinder the polymerization reaction.

Just before use the photo initiator solution was prepared dissolving Irgacure 2959 (Ciba) in methanol until saturation, which was found to corresponds to 350mg/ml slightly lower than the reported value in the datasheet of more than 50g in 100g of solution. In order to avoid deterioration of the photo-initiator this solution has to be shielded from light.

The prepolymer stock solution and the photo initiator solution are mixed in a 10:1 volumetric ratio immediately before UV exposure to limit the precipitation of Irgacure since the reported Irgacure 2959 solubility in water is 1g in 100g of solution, almost 50 times less than in methanol.

The solution composed by the prepolymer stock and the dissolved photo activator is thereafter referred to as photo-pattern solution.

2.1.3. UV exposure

UV exposure cleaves Irgacure molecules into free radicals catalyzing the free radical polymerization of acrylamide (figure 2.2.1), at the same time the radical polyacrylamide chain can react also with the silane groups on the treated glass surface binding the hydrogel to the glass.

The polymerization is carried out in a “sandwich” configuration as shown in figure 2.2.2a. A support glass slide is placed on the UV lamp tray, then a suitable amount of photo-pattern solution, for instance 100µl for a 25mm glass slide, is pipetted on it and the silanized glass is then place on top with the activated surface in contact with the photo-pattern solution and finally the photomask carrying the negative image of the desired pattern is placed on top. During the assembly care must be taken in order to avoid leakage of the solution. At this point the polymerization is started through UV exposure (OAI Lamp) using a 365nm wavelength and exposing for 90s (figure 2.2.2b)

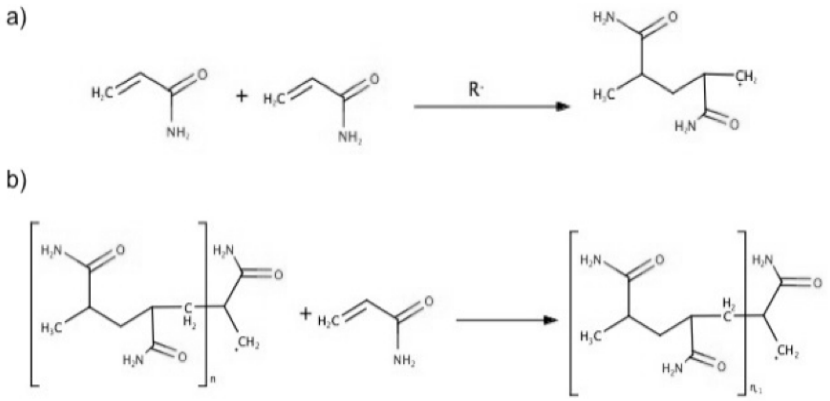

Figure 2.2.1. *The radical specie R, created by the interaction of UV light and a Irgacure molecule, initiates the reaction of two acrylamide monomers (a) starting the free radical polymerization of acrylamide (b).*

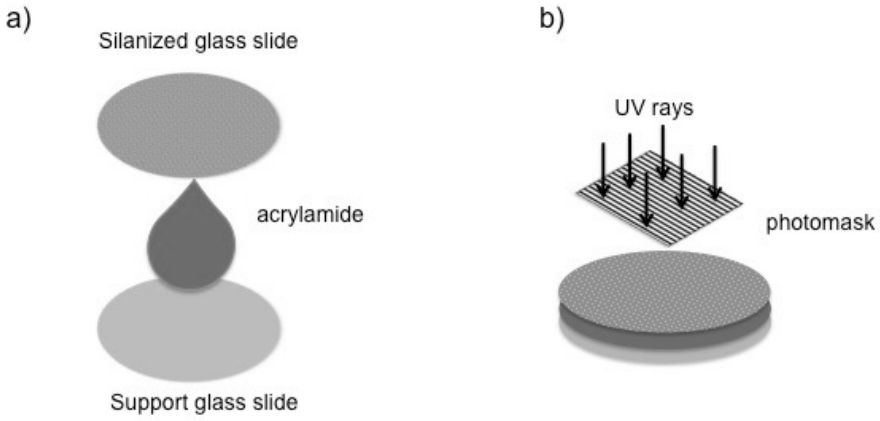

Figure 2.2.2 *Schematization of the sandwich preparation (a) and subsequent UV exposure (b) for the fabrication of photo-activated hydrogel pattern.*

Following the polymerization, the glass slides were left in a distilled water bath overnight to remove all unreacted acrylamides monomers that would be cytotoxic.

2.1.4. Substrate sterilization

Prior to cell seeding the substrates need to be sterilized. The bottom of the glass slides was sterilized with ethanol 70%$_{vol}$, laying the slides on a veil of ethanol for a few seconds and then posing them in a 6-well multiwell. Using ethanol on the functionalized surface was avoided for two reason: firstly, the ethanol would dehydrate the hydrogel shrinking it and possibly ruining the pattern efficiency and

secondly it could adsorb on the surface and interfere with cells adhesion. As a consequence, the upper surface of the glass slides was sterilized *via* UVC exposure for 25 minutes.

2.1.5. Fibroblasts culturing and seeding

In all the experiments performed to identify and optimize the patterning protocol Human Foreskin Fibroblasts (HFF) were used to initially check the effectiveness and efficiency of the technique. This choice was made because HFF are readily available, easy to culture among several passages and overall present a lower cost respect to terminally differentiated cells such as cardiomyocytes and smooth muscle cells.

HFF were cultured on 75mm^2 flask. The medium, composed of 89%$_{vol}$ DMEM 31966 (Thermofisher), 10%$_{vol}$ FBS (Thermofisher) and 1%$_{vol}$ Penicillin/Streptomycin (Thermofisher), was changed once every other day. Cells were passaged once 80% confluence was reached, to passage the cells the spent medium was aspirated and the flask was washed with PBS 1x (Life Technologies) and then incubated for 2 minutes with trypsin 0.25% (Sigma-Aldrich) to disrupt the proteins responsible of the cellular bounding to the culture flask and among each other. After the incubation, 10 ml of fresh medium were quickly added to block the enzyme action, afterwards a third of the cells suspension was re-plated in a new flask adding fresh medium until a total volume of 10ml was reached and the rest of the suspension was either used to test the patterned substrates or discarded.

For testing the patterned substrates cells were seeded ad high density (200 cells/mm^2, roughly one third of a confluent flask is sufficient for one one 6-well multiwell) to improve the probability of a cell to attach in the cell attractive areas. In this case after the cells were trypsinized an appropriate amount of cells suspension was collected, fresh medium was then added to the suspension to obtain a total volume of 2ml for every glass slide and finally 2ml of suspension was placed drop wise on every patterned glass slide. The seeded multiwells were then placed in the incubator,

carefully to avoid disrupting the drop and left still for 24 hours to allow cellular attachment. Once the cells were attached the patterned substrates were observed one day and one week after seeding to check the efficacy and efficiency of the protocol.

2.1.6. Glass photo-patterning results

Several trial on glass patterning through photo-activated acrylamide polymerization have been carried out. The obtained patterns presented very good spatial resolution, on the other hand the main problem experienced with this technique was reproducibility, meaning that even following the same procedure sometimes the pattern was achieved and others not.

To solve the issue of consistency in the results the patterning protocol was extensively reviewed highlighting the steps that might randomly change between different experiments and alter the acrylamide polymerization reaction.

Since the variability was observed even between glass slides produced in the same experiment, the reagents used for functionalizing the glass surfaces were always from the same bottle during the experiments and the acrylamide prepolymer was produced in batches, the variables left out were the photo-activator solution and the UV light exposure.

For what concerns the photo-activator solution, provided it has been handled correctly e.g. it has constantly been shielded from light, the inconstancy could depend on partial precipitation of Irgacure in the photo-pattern solution, since its solubility is lower in water than in methanol. To overcome this problem during the experiment the prepolymer solution was aliquoted and the photo-activator solution was added to each aliquot immediately before UV exposure to eliminate any lag time in the use of the photo-pattern solution and thus reduce the incidence of precipitation. Despite this expedient reproducibility was not significantly increased.

Having ruled out the photo-activator precipitation as a probable cause of the inconsistency of the results the focus was shifted on the UV exposure.

As described before (§2.1.3), the exposure time was kept fixed during the experiments and equal to 90s, however the UV lamp intensity might vary during prolonged use, in particular as the lamp heats up during usage the intensity decreases. As a result during the experiments, when many substrates were exposed one after the other, the actual total energy flux transferred to the polymerization reaction was varying. To address this issue firstly the optimal total energy flux was identified carrying out an experiment in which the exposure time was varied and the actual instant intensity delivered was recorded, the conditions that led to the best pattern were then used to determine the total energy flux required, which was found to be 630 mJ/cm^2. In the following experiments the intensity was recorded before each exposure and the exposure time was adjusted to obtain the desired energy flux.

Following this procedure, the consistency of the manufacturing protocol was increased, although some variability between slides still remained.

Since controlling the energy intensity at each exposure was time consuming, the results still showed heterogeneity and there is no way to check the success of the pattern prior to cell seeding, the photo-activate polyacrylamide pattern was set aside in favor of the chemical-activated polymerization described in the following paragraph.

2.2. Chemical activated polymerization

To overcome the reproducibility issues encountered with photoactivated polymerization the chemical activated polymerization of acrylamide was pursued.

In this case the acrylamide polymerization is a bulk process, so to achieve the desired pattern the cells attractive areas must be protected before creating the hydrogel. The areas that need to be acrylamide-free are sheltered by a layer of positive photoresist

deposited through standard photolithography techniques. The production process is summarized in figure 2.2.3

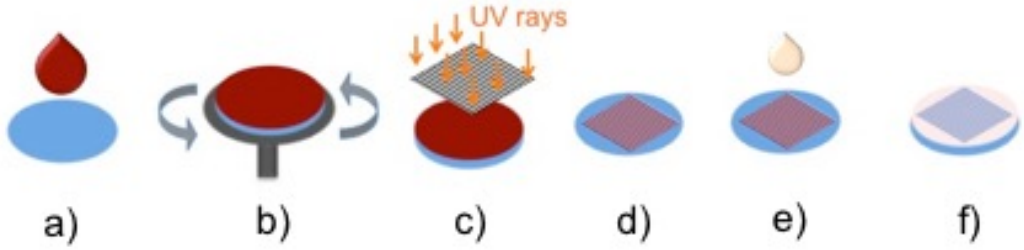

Figure 2.2.3. *Schematization of the photolithography-aided pattern: A drop of positive photoresist is deposided on the functionalized glass slide (a) and spinned to achieve desired thickness (b), the resist is exposed to UV light through a photomask (c) and the exposed resist is degraded and removed during developing (d). The acrylamide and chemical activators solution is deposited on the glass (e) and polymerized, finally the protective layer of resist is removed revealing the polyacrylamide pattern(f).*

The need of an additional manufacturing steps lengthens the production process, anyways this drawback is compensated for by higher reliability and higher throughput, since slide scan be produced in batches.

2.2.1. Glass preparation

The glass preparation comprises thorough cleaning of the surface using a piranha solution and functionalization of the glass surface with silane groups and follows the same steps described previously for the photo-activated acrylamide polymerization (§2.1.1).

Usually to promote the photoresist adhesion to the substrate the surface needs to be functionalized with hexamethyldisilazane, anyways in this case it was noticed that the absence of primer treatment didn't diminish photoresist adherence, at least for the application needed, so this step was omitted in the optimized manufacturing protocol.

2.2.2. Photolitography

During this fabrication step the cell adhesive areas are protected depositing a layer of resist. In this case S1800G2 (Microposit) photoresist was used. S1800G2 is a positive

photoresist, meaning that the portion of resist exposed to UV light is degraded and becomes soluble in the photoresist developer, so, as in the photo-patterning, the photomask has to cover the cell attractive areas.

Since the resist is photodegradable it has to be shielded from direct light until the development is completed, moreover afterwards the slides where covered in aluminum foil whenever possible to avoid deterioration until the protective layer of resist was removed.

The glass slides were placed in a spin coater (Laurell Technologies) to obtain a uniform layer of photoresist. A drop of resist was deposited in the center of the glass slide as to cover about 1/3 of the surface and spinned according to the following program to obtain a final thickness of 3µm:

Time (s)	**Speed (rpm)**	**Acceleration (rpm/s)**
7	2000	10000
1.5	1500	5000
30	3000	10000
10	1500	10000
5	2000	10000

Since the resist is only used as a protective layer the final thickness was not relevant, therefore the minimum height reliably reproducible was chosen to speed up the photolithography process.

The slides were then placed on a levelled hot plated heated to 115°C for 60s to promote the photoresist crosslinking. Afterwards the slides were placed in the UV lamp tray (OAI Lamp) and covered with the photomask, to ensure perfect flatness of the mask another glass slide was placed on top. The resist was exposed for 30s at 5mW/cm^2, giving an energy flux of 150mJ/cm^2, a value consistent with the manufacturer's suggestions.

Following the exposure, the slides were placed on the hot plated at 115°C for 60s and finally they were developed.

The developer used was the MF-319B (Microposit), expressly indicated to use with S1800G2 resist. The glass slides were dipped in the resist for about 20s and then rinsed with water, the obtained pattern was then observed with the aid of a microscope and the development was repeated, if needed, until all the resist was removed from the cell repulsive areas. This stepwise approach to development was adopted to limit the exposure to the developing solvent and avoid removal also of the cured photoresist.

2.2.3. Hydrogel polymerization

Having protected the cells adhesive areas with the resist it was possible to perform a chemically activated polymerization of acrylamide to generate the cell repulsive areas. The chemical patterning solution was composed of the linear acrylamide prepolymer solution described in §2.1.2 and degassed for 20 minutes to strip away dissolved oxygen molecules, ammoniumpersulfate (APS) as initiator and tetramethylethylenediamine (TEMED) as catalyzer in a 1000:10:1 volumetric ratio. As soon as the chemicals are mixed together they start reacting so it is necessary to use the solution quickly. A 100µl drop of solution was deposited on each glass slide and a cover slip was placed on top to spread the liquid evenly. The acrylamide free radical polymerization was completed in 20 minutes, after which the glass coverslip was carefully removed and the glass slides with the polyacrylamide hydrogel was placed in a water bath overnight to remove all unreacted acrylamide monomers.

2.2.4. Resist removal

Finally the protective layer of resist could be removed, to this end the glass slides were dipped in pure acetone until all the cured photoresist was removed and then thoroughly washed with deionized water.

Following this step, the polyacrylamide pattern on the glass slide is finally completed and the substrates can be sterilized and used for cell culturing as described previously (§2.1.4 and §2.1.5).

2.2.5. Glass chemical patterning results

Also in this case the first trials were carried out using HFF cells. Using this manufacturing process the pattern showed a good resolution, as with the photo-patterning, and in this case reproducibility was close to 100%. Moreover, following this production protocol, it is possible to verify prior to cell seeding if the acrylamide polymerization was successful, and therefore whether the pattern will be obtained.

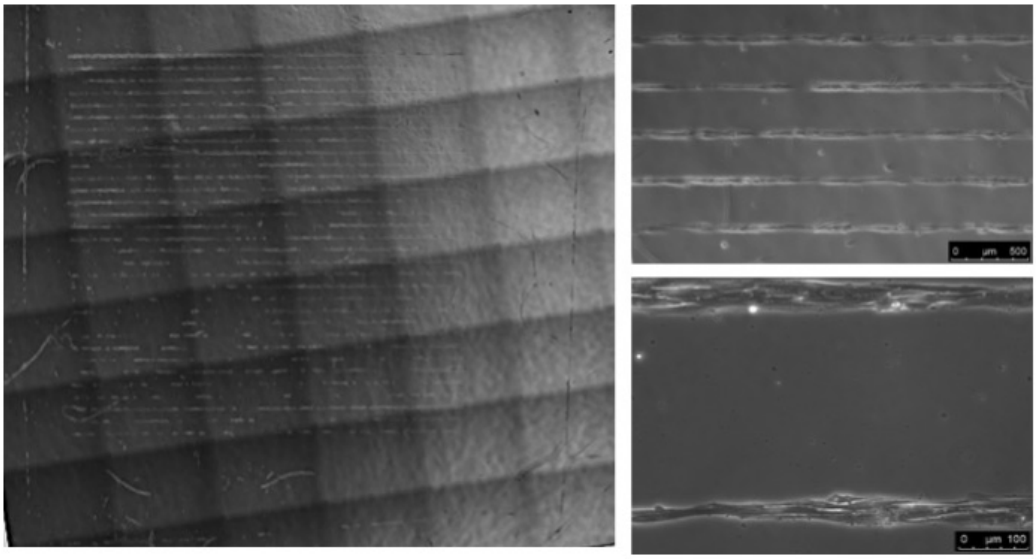

Figure 2.2.4 *Linear pattern of seeded HFF cells. On the left is depicted the whole patterned surface to show the overall results, while on the right two different zoom ins are presented to highlight the pattern definition. Nominal dimension of the pattern is 50µm wide lines spaced by 250µm.*

In figure 2.2.4 is reported an example of HFF linear pattern on glass slides obtained through chemical polymerization of acrylamide. On the left side the entire patterned surface is depicted, showing a good resolution of the pattern throughout the glass slide, in some areas the lines are not continuous, most likely this is due to an uneven distribution of cells during seeding. On the right side two enlargement are presented

to better appreciate the achieved pattern definition, it can be seen that the cells are highly aligned and constrained in the desired geometry.

Given the higher consistency of this techniques and the unvaried spatial resolution, chemical patterning through photolithography was preferred over photopatterning on glass.

2.3. Experiments with cardiomyocytes

The main purpose of developing glass patterning techniques was to allow electrophysiology studies of aligned cardiomyocytes and to analyze in depth the physiology of organized cardiac junctions. To this end it is necessary to culture cardiomyocytes on the patterned substrates.

2.3.1. Substrate functionalization

Contrary to fibroblast, cardiomyocytes require a suitable protein coating, usually laminin or matrigel, in order to adhere to any surface. Initially the coating was performed using laminin, preferred over matrigel since its composition is defined but it was later verified that both protein coatings show the same results.

To perform the coating a solution of laminin (Sigma-Aldrich) in PBS at 100µg/mL concentration or of Reduced Factor Matigel (Corning) diluted in Ham F12 Nutrient Mixture (Gibco) at 2.5% was deposited on the surface drop wise in order to cover all the surface and left incubating for 1 hour at 37°C. Afterwards the excess solution was removed and the substrates were ready for cell seeding.

2.3.2. Cardiomyocytes seeding

Cardiomyocytes seeded on the patterned surfaces were derived from pluripotent stem cells and maintained following the procedures already established in the laboratory (Martewicz 2015).

Prior to seeding the cardiomyocytes were incubated with 10µM of ROCK inhibitor (Y-27632, StemCell Technologies) for 75 to limit dissociation induced cell apoptosis.

Once the inhibitor incubation time is elapsed, the medium is aspirated from the cell culture and the cells are washed for 2 minutes with $PBS^{-/-}$, which is PBS without Ca^{2+} and Mg^{2+}, (Gibco). Afterwards the $PBS^{-/-}$ is aspirated and the culture is incubated for 25 minutes with a digestion mix made of 2mg/ml collagenase I (Thermofisher Scientific), 1mg/ml collagenase IV (Thermofisher Scientific), 2 U/ml Dnase I (Thermofisher Scientific) and 10µM ROCK inhibitor in $PBS^{+/+}$ (Gibco).

After the incubation the digestion mix is removed and cells are incubated for 4 minutes with Triple Select (Thermofisher Scientific). The cardiomyocytes are then re-suspended through vigorous pipetting of the solution. Immediately after detachment of the cell monolayer, the STOP medium, composed on 50% DMEM and 50% FBS and 2U/ml DNase I, and is added.

The cell suspension is then centrifuged for 5 minutes at 1200rpm to allow the removal of the supernatant from the cell pellet and finally cells are suspended in RPMI (Thermofisher Scientific) supplemented with B27 (Thermofisher Scientific), the standard culture medium for cardiomyocytes, and seeded on the substrates.

2.3.3. Results and troubleshooting

When cardiomyocytes were seeded the pattern was no longer present on the glass slides, since the only difference with the trial experiments using HFF was the need of a protein coating it was suspected that somehow the protein interacted with the hydrogel erasing the difference between cell attractive and cell repulsive areas.

To solve this problem other trials employing HFF cells and a protein coating such as the one required by cardiomyocytes were performed to identify what was causing this interaction.

After several modifications of the manufacturing protocol it was discovered that adding a small quantity of bis-acrylamide in the prepolymer solution enabled the hydrogel to withstand the protein coating.

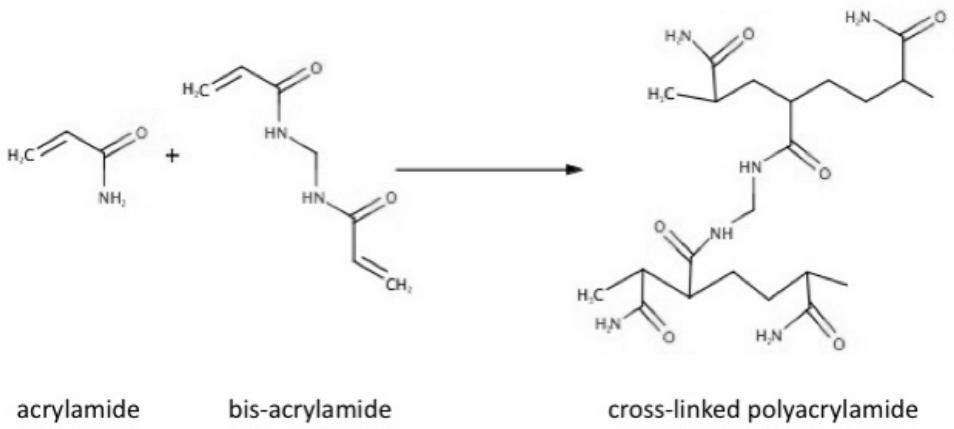

Figure 2.2.5 *The addition of bis-acrylamide in the prepolymer solution allows the formation of a crosslinked gel binding different polyacrylamide chains together.*

As shown in figure 2.2.5, the addition of bis-acrylamide causes the formation of a crosslinked hydrogel, the ratio between linear and bis-acrylamide determines the extent of the crosslinking and thus the gel stiffness. In order to maintain an high stiffness difference between adhesive and repulsive area, the lowest amount of bis-acrylamide that allowed to withstand protein coating was used, which was found to be 0.12% of the total solution volume.

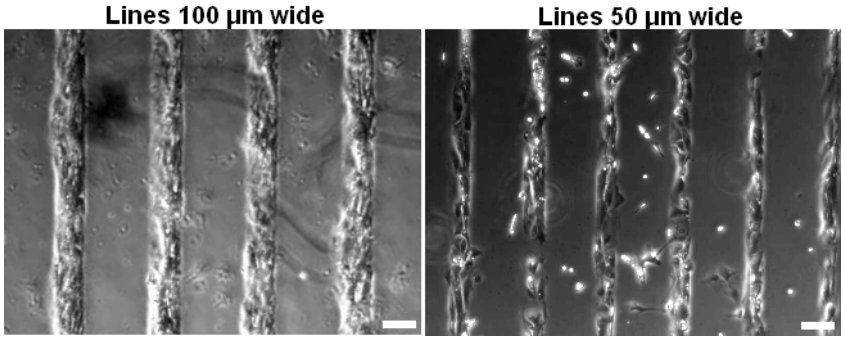

Figure 2.2.6 *Linear patterning of cardiomyocytes on glass. (Adapted from Martewicz 2015).*

The final production method developed for patterning on glass uses photolithography as a way to create the desired pattern, which is made of slightly crosslinked chemically activated polyacrylamide. This procedure allowed to produce reliably patterned glass

slide for culturing aligned cardiomyocytes as shown in figure 2.2.6 and can now be used to study in detail the physical and electrical coupling of cardiomyocytes.

3. PDMS patterning

Techniques to realize a geometrical pattern on elastomeric substrates have been implemented to be coupled with the stretching technologies developed during this work, and described in the following chapter, in order to perform mechanical stimulation of aligned cells, explicitly stressing the cellular junctions.

PDMS has been selected as the elastomeric material since it is widely use in biologically experiments, its mechanical properties are defined and was already used and known in the laboratory.

There are two different approaches to patterning on PDMS: one is to perform a chemical pattern, employing the same principle adopted for glass patterning; the other one is to realize a physical pattern made of PDMS channels of different height.

In the following paragraph both methods will be described, presenting the results obtained and their integration with the stretching technologies.

3.1. Physical PDMS patterning

Physical patterning of PDMS consist in creating grooves on the substrate surface that direct cell orientation by creating a physical constraint, as schematized in figure 2.3.1.

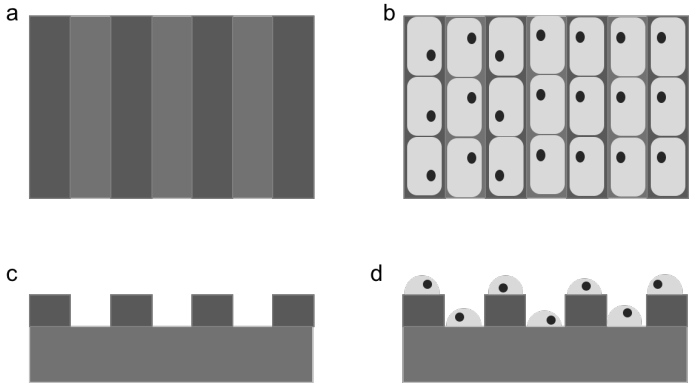

Figure 2.3.1 *Schematic representation of physical PDMS patterning. Grooves of PDMS ore realized on the surface (a top view, c side view). Seeded cells arrange on the different layers and are forced to align (b top view, d side view).*

The principle underlying this patterning technique is quite naïve, and also its realization is straightforward. The only issue lays in its integration with the stretching systems, as the additional channels of PDMS change the substrate mechanical properties, requiring additional force to obtain a given deformation. This doesn't affect the function of the mesofluidic stretching device described in chapter 3 §2, since the machine providing the mechanical stimulation can easily overcome the concern, but renders the technique inapplicable with the microfluidic stretching device described in chapter 3 §3, and for this reason also chemical patterning of elastomeric surfaces has been developed.

3.1.1. Mold preparation

To perform the pattern on the surface first a PDMS stencil presenting the negative of the desired pattern needs to be obtained. The stencil is obtain through replica molding from a mold, in this work the mold was a 4" silica wafer (Siegert-wafer) on which the desired pattern is realized through soft-litography.

Briefly the wafer is cleaned with methanol and ethanol and finally rinsed with milliQ water to remove al residues from the surface. The wafer is then placed on the spin coater (Laurell) and a negative photoresist is poured on it as to cover 1/3 of the surface. In this case the height of the features isn't relevant for the final use, so it was kept low to speed up the production process. SU8 2005 was used to obtained a final resist height of 6µm, determined by setting the spinning program as follows:

Time (s)	Speed (rpm)	Acceleration (rpm/s)
10	500	100
30	2000	300

Afterwards the wafer was left on a levelled plane for 2 minutes, to remove residual tension in the resist, and then placed on a levelled hotplate (Torrey Pines Scientific) at 95°C for 2 minutes as specified by the manufacturer's manual.

Subsequently, the wafer was placed in the UV lamp tray (OAI), and was exposed to UV light at 365nm for a total exposure energy of 110 mJ/cm^2 through a suitable

photomask carrying the features of the desired pattern to cure the polymer exposed to UV radiation. The wafer was then placed on the hot plate for another 3 minutes and finally it was developed in a bath of methossimethacrilate (Sigma-Aldrich) for 3 minutes. It was then rinsed with iso-propanol (Sigma-Aldrich), the alcohol reacts with uncured resist forming milky residues, in the presence of such residues the wafer was placed back in the methossimethacrilate bath for another minute and the process was performed until all uncured resist was removed. At this point the mold is ready to be used.

3.1.2. Stencil fabrication

Having obtained the mold, it is possible to fabricate the PDMS stencils. At the first use, and afterwards about once every 10 times, the wafer is treated with hexamethyldisilazane (HDMS, Sigma-Aldrich) to promote the detachment of the PDMS from the wafer. To this end a few microliters of HDMS are placed with the mold in a low pressure environment, about 10^1 mbar, for half hour to allow for the chemical evaporation a redistribution on the surface. Afterwards uncured PDMS, obtained mixing Sylgard 184 base and curing agent at a 10:1 weight ratio and mixing thoroughly, is poured on the surface and extensively degassed to strip away all air bubbles. The wafer is then placed in a convection oven for 1 hour at 80°C, or overnight at 40°C to promote crosslinking of the polymer. Afterwards the PDMS is extracted from the mold and the stencil is ready.

3.1.3. Physical pattern fabrication

The stencils are treated with a perfluorinated trichlorosilane (T2492-KG, UCT Specialties) to prevent the adhesion of PDMS on them during the patterning. To this end, the stencils were placed in a vacuum container with the engraved surface facing up and a few microliters of the silane were added. The pressure was then reduced to about 5 mbar to enhance evaporation of the chemical, and the stencils were left in perfluorinated trichlorosilane vapours overnight.

Afterwards, uncured PDMS in a 10:1 base to curing agent ratio was deposited on the treated stencil surface in order to cover it completely with a veil of pre-polymer, after a quick passage in the vacuum chamber to remove air bubbles that may remain trapped in the grooves, the stencil was firmly pressed on the PDMS surface on which the pattern is needed and placed on a hotplate at 100°C for one hour. When the thin layer of PDMS between the stencil grooves and the to-be-patterned surface is cured, the stencil can be removed, peeling it off delicately. Thanks to the treatment with the fluorinated silane, the newly cured PDMS will not bind to the stencil PDMS, but only to the surface, creating the desired pattering groove.

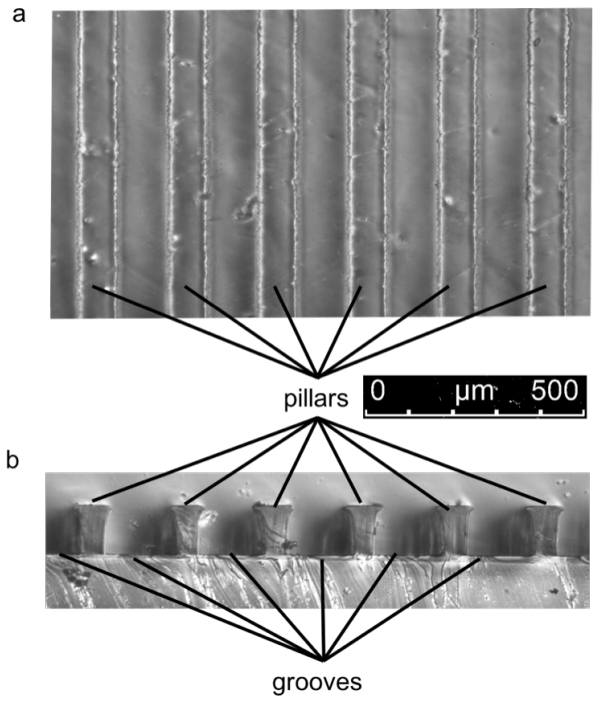

Figure 2.3.2 Top view (a) and *transversal section (b) of a PDMS surface with a linear physical pattern. The grooves, corresponding to areas where the second layer of polymer was squeezed out by the stencil, are clearly distinguishable from the pillars, linear channel formed during the curing of the second layer of polymer.*

A picture the linear pattern obtained through this method is reported in figure 2.3.2, the two different layers over which the cells will attach, marked as grooves and pillars

on the picture, can be easily distinguished looking both at the top view (2.3.2a) at the cross section (2.2.3b) resembling the scheme reported in figure 2.3.1 c and d.

The treated stencils can be reused several times, after many cycles, however, small pieces of PDMS tend to stick also to the treated surface clotting the grooves, so periodically it is necessary to produce new ones to ensure a good pattern reproducibility.

3.1.4. Surface sterilization and functionalization

Prior to biological experiments the substrates had to be sterilized following the procedure described in §2.1.4.

Once sterilized, the surface needs to be functionalized through a protein coating since cells don't naturally adhere to PDMS.

During the trial experiments the functionalization was performed with Reduce Factor Matrigel as described in §2.3.1.

3.1.5. Results

The efficacy of this technique was firstly tested using HFF cells following the procedures described in §2.1.5.

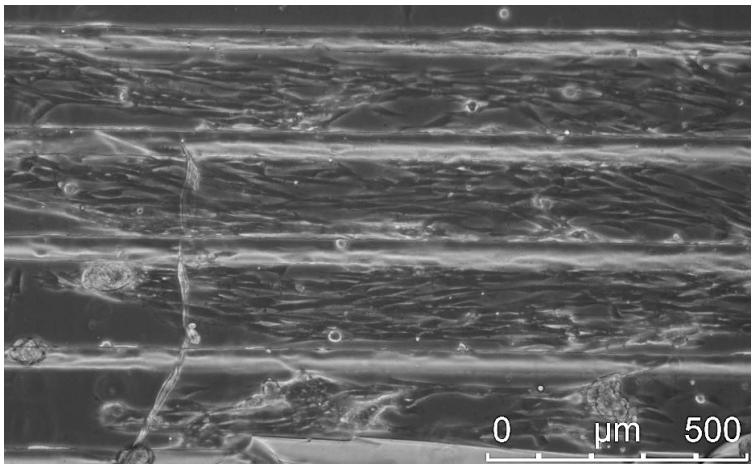

Figure 2.3.3 *HFF cells seeded in a PDMS substrate with physical linear pattern.*

The results obtained seeding HFF at high density on a surface with a linear pattern with 50µm wide pillars and 250µm grooves are reported in figure 2.3.3.

In the image the arrangement of cells both on the grooves and on the pillars can be seen, and the effect of the physical constraint on cell alignment is quite evident, even though the groove width is much larger than the size of the cells.

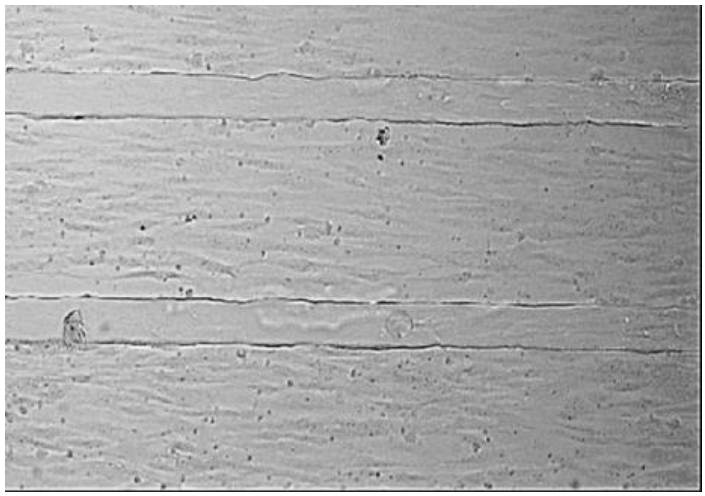

Figure 2.3.4 *Human myoblasts seeded on the linear patterned substrates*

.

In figure 2.3.4 a representative picture of the results obtained seeding human myoblasts on the patterned substrate is reported. It can be seen that also in this case the cells tend to aligned along the grooves direction despite the pattern being larger than cells dimensions.

3.1.6. High density cardiomyocytes seeding

Since the major aim of the patterning techniques developed is to obtained alignment and polarization of cardiomyocytes, the compatibility of the physical PDMS patterning with that specific cell line has been tested.

The purpose of developing patterning techniques on elastomeric substrates such as PDMS is to analyze the response of cells when their junctions are subjected to mechanical strain. To obtain highly organized and polarized junctions, that mimic the *in vivo* physiology, it is necessary to seed the cardiomyocytes at high density in order to obtain an almost confluent monolayer, moreover the stencils had to be modified in

order to obtain grooves and channels of 50µm, to ensure cardiomyocytes orientation on both layers.

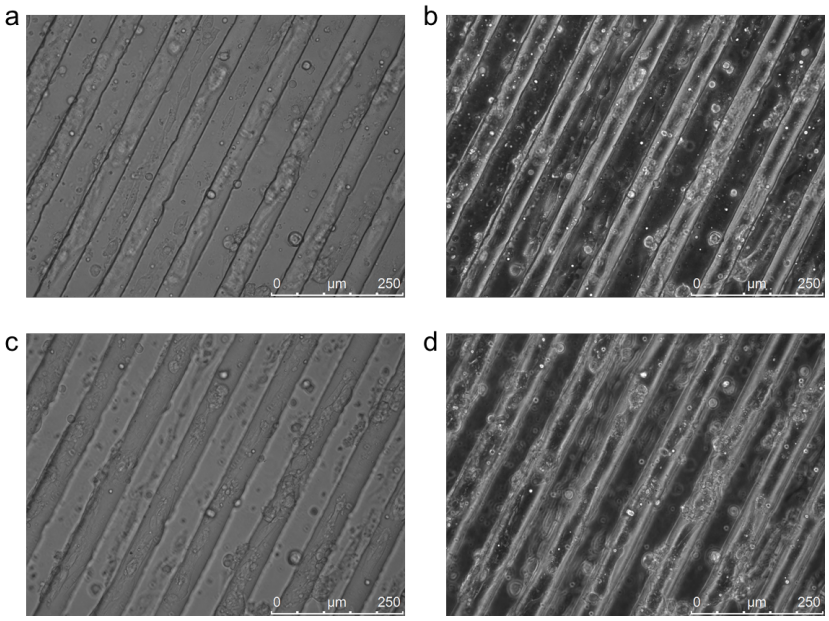

Figure 2.3.5 *Cardiomyocytes seeded on the physical linear patterned PDMS. Cells aligned both on the pillars (c bright field, d phase contrast) and in the grooves (a bright field, b phase contrast).*

The cardiomyocytes were prepared as described previously (§2.3.2) and seeded on the PDMS substrates with physical linear pattern. As can be seen from figure 2.3.5, the cardiomyocytes align both on the pillars and in the grooves, giving rise to linear stripes of cardiomyocytes resembling physiological conditions of the gap junctions. This technology can now be used to reproduce *in vitro* the cardiac junction and subject it to controlled mechanical strain to study the effect of uniaxial stress both in healthy and diseased cardiomyocytes.

3.2. Chemical PDMS patterning

Chemical patterning of PDMS consists in realizing cell repulsive areas constituted by a layer of polyacrylamide, as in the case of glass patterning. Based on the experience gained developing patterning techniques for glass substrates (§2.3.3), also in this

application a slightly crosslinked hydrogel was created adding 0.12% of bis-acrylamide in the acrylamide solution.

The necessity of developing a second technique to pattern elastomeric substrates arose from the limited applicability of the physical pattern just to stretching systems for which the force necessary to obtain a given deformation isn't an issue. As mentioned in §3.1 the chemical PDMS patterning is specifically designed to be coupled with the microfluidic technology to culture cells in mechanically active conditions developed during this work and described in the following chapter.

This technique was developed and optimized using PDMS round slabs of 12mm diameters, punched from a 100µm thick membrane of PDMS at a 10:1 weight ratio of base and curing agent, placed on a 12mm diameter glass slide. This was done to mimic as closely as possible the actual conditions of pattering a microfluidic device, without using directly a completely formed microfluidic chip as it would be more time consuming and costly.

3.2.1. Benzophenone insertion

As in the case of glass patterning, it is necessary to provide some anchoring points on the surface so the forming polyacrylamide chain can bind to it.

In this work benzophenone was used as anchoring point, modifying the protocol reported by Simmons and coworkers (Simmons *et al*. 2013).

Benzophenone can be inserted inside the cured PDMS network by acetone induced swelling, in this work benzophenone was dissolved in a solution of 80%$_{vol}$ acetone (Carlo Erba) and 20%$_{vol}$ milliQ water, reaching a final concentration of 10% by weight. The glass slides with the PDMS slabs were placed inside a glass petri dished and chilled for 15 minutes at +4°C, afterwards the petri was placed on ice and a 60µl drop of benzophenone solution was pipetted on each PDMS slab. The petri was then covered and placed in the fridge at +4°C for 60 minutes. The benzophenone insertion was carried out at low temperature to reduce acetone evaporation and allow longer

reaction time, if the process is conducted at room temperature, within 2 minutes the acetone drop is already completely evaporated.

Afterwards the PDMS slabs were dipped in a methanol bath and dried with a flux of nitrogen.

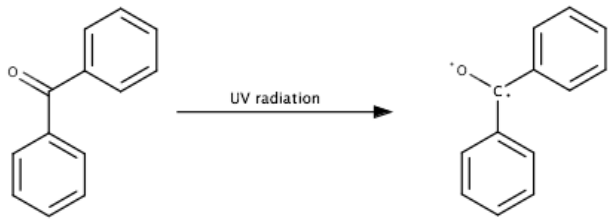

Figure 2.3.5 *Benzophenone irradiated by UV light forms a highly reactive bi-radical.*

Benzophenone, irradiated with UV light, forms a bi-radical molecule (figure 2.3.5, that in turn can react with the acrylamide polymeric chain, since the benzophenone itself is not chemically bind to the PDMS, this creates an interpenetrating network of polymers.

Since the benzophenone is activated by UV radiation, and consequently can be selectively activated on the PDMS surface by exposure through a photomask, the acrylamide polymerization can be activated both chemically and photo-chemically.

3.2.2. Acrylamide chemically activated polymerization

Since the chemical activation of acrylamide gave the best results in the glass pattering studies, it was the first method employed also for the chemical patterning of elastomeric substrates.

The acrylamide solution was prepared as described previously (§2.2.3), with the addition of 0.12% of bis-acrylamide.

The polymerization was carried out in a “sandwich” configuration, as represented in figure 2.2.2, placing a 12mm diameter glass slide in the UV lamp tray (OAI), a 10µl drop of acrylamide solution, completed with APS and TEMED just before use, and the glass slide with the benzophenone-treated PDMS slab facing downwards, finally, on top of

the glass slide was placed the photomask with the pattern design. The UV lamp was then switch on performing the benzophenone activation simultaneously with the acrylamide chemical polymerization.

After 20 minutes the polyacrylamide reaction is completed so the UV radiation was switch off and the sample was removed. The support glass slide was discarded while the one with the PDMS slab was placed in a water bath overnight to remove all unreacted acrylamide monomers.

3.2.2.1. *Results*

The PDMS slabs were sterilized and functionalized as described previously (§3.1.4) and, as a trial to check the efficacy of this method, HFF cells were seeded following the protocol reported in §2.1.5.

As can be seen in figure 2.3.6, the linear pattern can be clearly seen on the PDMS surface, but the cells were unable to attach to the substrate.

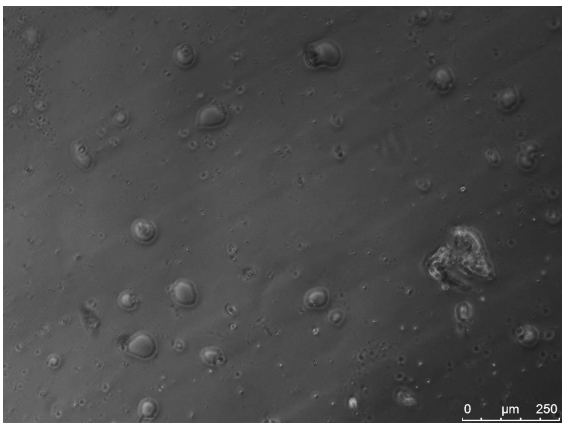

Figure 2.3.6 *HFF seeded on PDMS with chemically activated acrylamide polymerization. The linear pattern can be seen of the surface but the cells fail to adhere to the substrate.*

A possible explanation is that the chemically polymerized cross-linked hydrogel is actually formed all over the surface, and held in place by the binding to the activated benzophenone in the patterned areas. The same thing didn't occur in the case of chemically polymerized acrylamide on glass because in that case the

resist protecting the cell adhesive areas constituted a physical barrier that impeded the formation of a uniform layer of hydrogel.

For this reason, chemically activated polymerization of acrylamide was discarded in favor of photo-chemical polymerization.

3.2.3. Acrylamide photo-chemically activated polymerization

The acrylamide solution for the photo-chemically activated polymerization was prepared as in the case of glass patterning (§2.1.2) with the addition of 0.12% of bis-acrylamide. For the UV exposure the same "sandwich" configuration as before was used. The benzophenone was pre-activated, exposing it to UV light trough a photomask for 20 minutes, then a 10µl drop was added between the support glass slide and the PDMS and the exposure was continued for another 150s.

Afterwards the support glass slide was discarded and the PDMS slab was placed in a water bath overnight to remove all unreacted acrylamide monomers.

3.2.3.1. *Results*

The PDMS slabs were sterilized and functionalized as described previously (§3.1.4) and, as a trial to check the efficacy of this method, HFF cells were seeded following the protocol reported in §2.1.5.

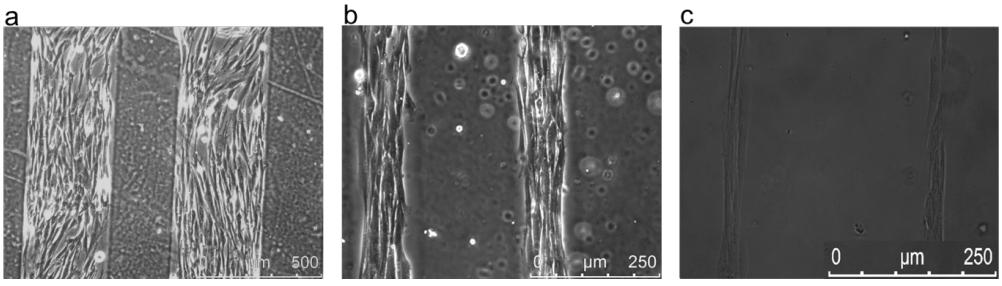

Figure 2.3.7 *HFF cells seeded on chemically patterned PDMS. Different line widths were realized ranging from 300µm (a), to 100mµ (b) and finally 50µm (c).*

As shown in figure 2.3.7, the polymerization of the gel restricted to the cell repulsive areas combined with the selectively activation of benzophenone allowed to seed cells along the linear pattern. The technique can be used to obtain a variety

of shapes and dimensions, in figure 2.3.7 the obtainment of linear patterns of 300µm (a), 100µm (b) and 50µm (c) is reported.

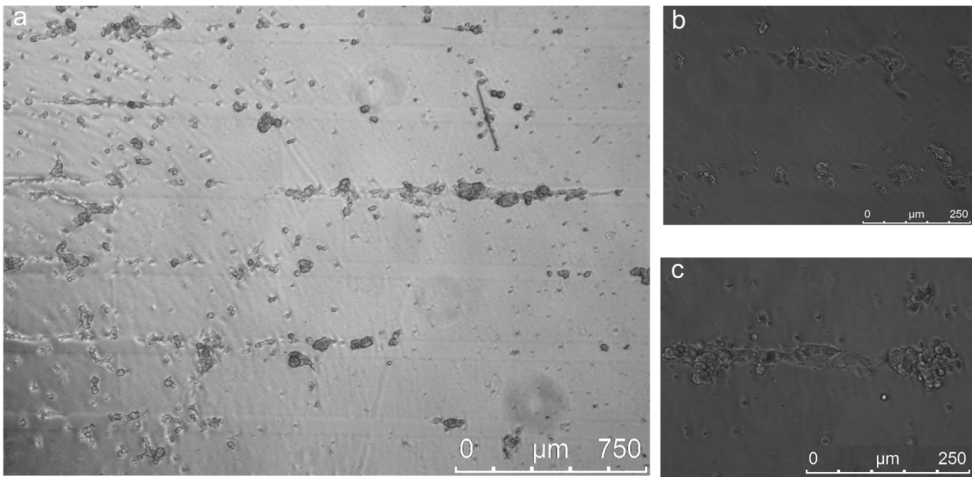

Figure 2.3.8 *Cardiomyocytes seeded on chemically patterned PDMS.*

The chemical PDMS patterning through combined photochemical polymerization of acrylamide and photo-activation of binding sites has been tested also with cardiomyocytes in view of future stretching experiments of aligned heart muscle cells. The cardiomyocytes were prepared and seeded on the patterned PDMS slabs as described previously (§2.3.2).

Figure 2.3.8 proves that the established technique allows to create linear pattern of cardiomyocytes on elastomeric substrates with good reliability. Prior to perform the stretching experiments on aligned cardiomyocytes the seeding conditions needs to be optimized, especially regarding seeding density, to avoid the presence of void spaces in the pattern as can be seen in figure 2.3.8.

3.2.4. Patterning stretchable devices

The chemical patterning technique for elastomeric substrates has been developed with the intent of coupling it with the microfluidic stretching device described in chapter 3, §3. Once the manufacturing protocol has been tested and optimized using PDMS slabs and HFF cells, it was transferred to the actual microfluidic chip.

All the manufacturing steps are the same as described previously (2.3.3), the only difference lays in the sandwich configuration for UV exposure, that had to be slightly modified since the device has an outer holding ring. In this case the 10µl drop of acrylamide photo-pattern solution was pipetted in the center of the device's culturing area, the support glass slide was then placed on top to evenly spread the drop and finally the device was tilted to perform the UV exposure, the capillary force between the aqueous solution and the glass prevented the detachment of the latter during the exposure.

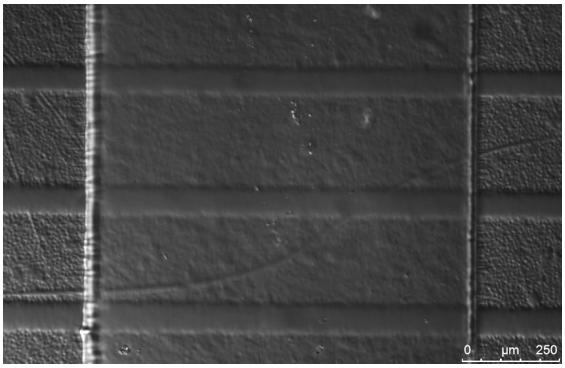

Figure 2.3.9 Linear pattern of polyacrylamide formed across a stretching chamber of the microfluidic stretching device. The pattern forces cells to align parallel to the main direction of deformation.

In figure 2.3.8 a linear pattern obtained on the PDMS surface of a microfluidic stretching device is reported. In the center of the picture it is possible to see the stretching chamber, while the linear pattern is perpendicular to the edge of the chamber. In this way the linear pattern directs the alignment of the cells parallel to the main direction of deformation of the stretching device, allowing to study the effect of mechanical strain on cellular junctions.

4. Final Remarks on patterning techniques

During this work patterning techniques both for rigid and elastomeric substrates have been developed and optimize especially with regard to their application in the study of the cardiovascular system.

For what concerns patterning glass surfaces, it was shown that chemically activated acrylamide polymerization, coupled with soft-lithography, provides the best results in terms of pattern resolution and reproducibility. Furthermore, it was discovered that the addition of a small percentage of bis-acrylamide, and therefore the formation of a crosslinked cell repulsive hydrogel, gives better results, especially when protein coatings are needed.

Glass patterning will allow to study the physiology of organized cardiac junctions in a highly polarized cell culture, that reproduces with higher accuracy the *in vivo* environment. Moreover, the alignment of cardiomyocytes will allow also electrophysiology studies on the propagation of the electrical signals among cardiac cells, analyzing in detail the intercellular electrophysiological coupling. Finally, this technology will allow to study the effect of morphology, shape and polarization in specifying cell fate and behavior (Mc Cain and Parker 2011).

The development and optimization of patterning techniques for elastomeric substrates, specifically PDMS, was divided in two categories, aimed at different applications.

Firstly, the production of a physical pattern was optimized. In this case cell morphology is influenced creating grooves and pillars on the culturing surface. This methodology is straightforward and easy to apply and implement, on the other hand its integration with stretching technologies, which is the ultimate goal of patterning elastomers, is limited to the technologies for which the force required to achieve a given deformation isn't a major concern.

Secondly, to overcome the issue of limited applicability of the physical pattern, the realization of a chemical pattern on PDMS was studied and optimized. To establish this technique, the knowledge acquired during the refinement of glass patterning was exploited, especially for what concerns the hydrogel composition.

PDMS patterning will allow to couple mechanical stimulation and alignment, closely mimicking the actual *in vivo* conditions and opening the way to groundbreaking studies on the electromechanical coupling, especially of cells of the cardiovascular system.

Chapter three
Stretching Systems

The second main topic of the doctoral research was the development of devices to enable cells culturing in mechano-active environments. The cardiovascular system is characterized by constant cyclic mechanical stretch throughout the life of a person so, to replicate *in vitro* the *in vivo* environment and obtain further insight of the mechanism involved in the physiological and pathophysiological response of the cardiovasculature, it's important to be able to reproduce also the distinctive mechanical cues faced by cardiomyocytes and vascular cell lines.

During the thesis two different devices to cyclically stretch cultured cells, that addressed distinct biological assays, were developed and tested.

In this chapter the mechanical environment of the heart and the cardiovascular system will be briefly discussed, setting the design requirements for the stretching systems. Then the development of the two stretching devices will be described. For each of the two developed devices the design and the production steps will be described, then the experiments performed to validate the new technologies will be presented, focusing both on the experimental set up and on the results obtained. Finally, the results obtained with both newly developed devices will be discussed with a global point of view, elucidating how the features of these new technologies can be exploited to expand the current experimental capabilities and deepen the knowledge in the biological response to mechanical *stimuli*.

1. Mechanical requirements of the cardiovascular system

Mechanotransduction is the process by which external mechanical factors are transduced in chemical and electrical signal by the cells. Despite all cells, in physiological conditions, are able to sense and react to such external *stimuli,* this process gains particular relevance in the case of tissues and cells that are constantly subjected to mechanical strain *in vivo*, as in the case of the heart and the circulatory system.

Designing the technologies to reproduce the unique mechanical conditions typical of the cardiovascular system it is essential to clearly define the frequency and elongation that the devices have to guarantee in order to represent the *in vivo* conditions.

In the heart typically cells are subjected to cyclic stretch at 1Hz frequency, which corresponds to 60 beats per minute, higher frequency is usually associated with physical strain but the majority of the *in vitro* models realized to re-enact cardiac mechanical conditions work at 1 Hz frequency (Dan *et al* 2015, Salameh *et al* 2010) For this reason, also in this work the systems were designed, and tested, to work at 1 Hz frequency, even though higher values could be achieved either simply changing the setting of the computer controlled stimulation, as in the case of the mesofluidic stretching device describe in §2, or by minor adjustments of the experimental set up, as in the case of the microfluidic stretching system described in §3.

For what concern the elongation imposed to the cells the values reported in the scientific literature are more widespread, mostly ranging between 5% and 20% (Dan *et al* 2015, Salameh *et al* 2010, Schmelter *et al* 2006). During this work we considered a physiological level of stretch for cardiomyocytes of 15%, and the systems have been designed to allow an elongation of 20% to reproduce also pathological conditions that have been shown to affect cellular behavior leading hypertrophy.

The requirements of the vascular system are equal or less than those of the heart (Tarbell *et al.* 2014, Huang and Li 2008), so in the design specification were set in reference to the cardiac demands. During this work a cyclic stretch of 10% elongation at 1 Hz has been considered as a model of the vasculature physiological conditions.

2. Mesofluidic stretching device

The bigger stretching device developed in this work has been named mesofluidic stretching device, since its feature aren't of the order of magnitude typical of microfluidic technologies, but on the other hand, the design, development and experimental phases resemble more closely those of microfluidics aided biology rather than classic biological techniques.

The main purpose of this device is to allow high-throughput analysis, such as RNA, DNA or protein expression analysis, of mechanically simulated cells cultures. All these biological techniques required a high number of cells from which the sample for analysis are obtained, thus the area devolved to cell culture needs to be quite wide, moreover since the whole cellular extract is analyzed together, the mechanical strain should be homogenous throughout the surface.

The cell culturing area was designed to be $9cm^2$, arranged as a square of side 3cm. If the necessity arises it is anyways possible to reduce the culturing area during cell seeding.

The downside of this newly developed experimental tool is that its size and mechanism of action prevent its compatibility with standard incubators, thus limiting the maximum duration of the mechanical exertion, despite an environmental control system has been developed to work alongside the mesofluidic stretching device.

The device was developed in collaboration with prof. Piero Pavan, University of Padua, and all experiments performed were carried out in collaboration with his laboratory.

In the following paragraphs the materials and methods employed to manufacture the mesofluidic stretching device will be described, then the results obtained using this newly developed technology will be presented and discussed.

2.1.Materials and methods

The mesofluidic stretching device is composed by a 1mm thick PDMS membrane that serves as a cells culturing substrate and an external holding ring also made in PDMS. The cyclic mechanical strain is applied through the ElectroForce® planar biaxial TestBench (Bose), in order to insert the device in the machine pincers, metal bars are tightly screwed

to the outer ring, moreover, to prevent possible contaminations during the experiments, another PDMS membrane in fixed on top the device during stimulation.

In figure 3.2.1a the different parts composing the mesofluidic stretching system are represented in an exploded view of the device. In figure 3.2.1b-c a picture of the device inserted in the stimulating machine, both from side and top view, is reported.

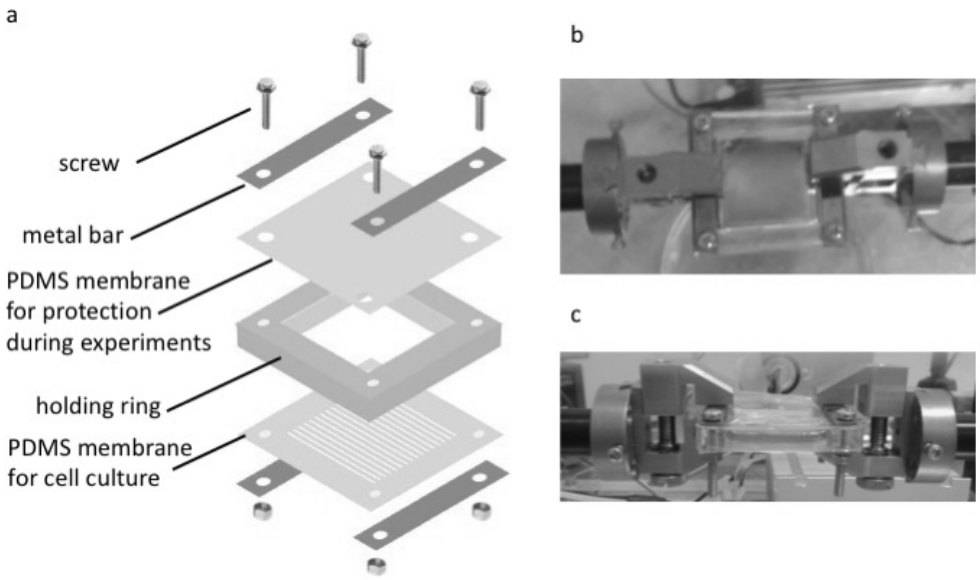

Figure 3.2.1 *Blown up representation of the mesofluidic stretching device to highlight the different parts composing it (a). Picture of the device integration in the ElectroForce® planar biaxial TestBench (Bose) showing the top (b) and side (c) views.*

As reported in figure 3.2.1, it is possible to create a linear pattern on the bottom PDMS membrane to obtain an aligned cell culture using the physical PDMS patterning techniques described in chapter 2, §3.2.

2.1.1. PDMS membrane preparation

The 1mm thick membranes are made of PDMS prepared mixing Sylgard 184 base and curing agent in a 10:1 weight ratio and pouring it in a rectangular petri dish of 10x10cm (Sarstedt). The desired thickness is such as to render impractical the use of a spin

coater to obtain a homogenous film, so the exact quantity of prepolymer required to obtain a 1mm layer on the receptacle was calculated.

The prepolymer was extensively degassed and then placed in a convection oven to promote PDMS curing, taking care that the oven trays were correctly levelled to avoid the obtainment of a membrane with uneven thickness.

Once cured the membrane was extracted from the petri dish and cut to the appropriate size, from each petri four membranes were obtained.

2.1.2. Holding ring fabrication

The holding ring carries out two functions: it creates a well-like culture system to facilitate cell culturing and it provides the coupling to the mechanical stimulation apparatus.

Also in this case Sylgard 184, with a base to curing agent weight ratio of 10:1 was used.

To ease the production step of the holding ring and obtain always exact pieces a poly(methyl methacrylate) (PMMA) mold, able to produce simultaneously four holding rings, was designed and produced.

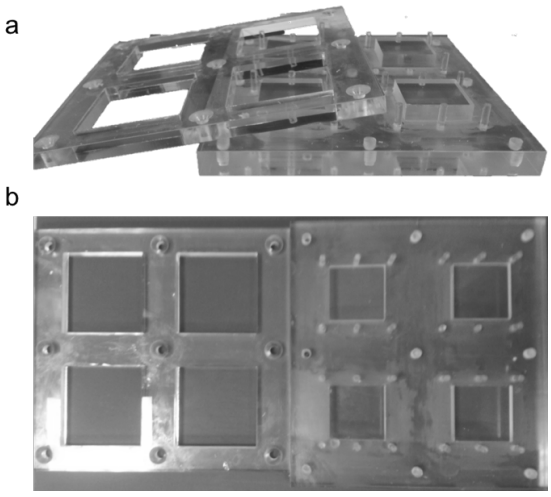

Figure 3.2.2 *PMMA mold used to fabricate the holding rings. Side view(a) and top view(b).*

As shown in figure 3.2.2, the mold is composed of two pieces: the bottom part carries the features to realize the central void dedicated to the cell culture and also spaced pillars of 3mm diameter to obtain the hole through which the screws are inserted; on the top part the outer limit of the ring is realized. The two pieces of the mold are tightly screwed together, and the prepolymer is poured in the hollow spaces, that reproduce the final form of the holding ring. The PDMS is degassed and finally cured in the convection oven for 4 hours at 60°C, afterwards the mold is opened and the holding rings are extracted.

2.1.3. Device assembly

The bottom PDMS membrane and the holding ring are irreversibly attached through plasma activated surface bonding. As previously described, the two pieces are placed in the plasma cleaner chamber (Herrick Plasma) with the surfaces that needs to be activated facing upwards, the pressure is reduced to $3*10^{-1}$ mbar and the plasma is activated. The PDMS surface is treated with plasma for two minutes, keeping the pressure constant for better performances, then the vacuum is released and the two pieces are bond together. The device is left on a levelled hot plate (FALC) at 100°C for 10 minutes to promote the irreversible bonding between the two pieces.

Afterwards, 3mm diameter holes are punched in the membrane in correspondence with the screw holes in the holding ring to allow the passage of the screws when needed.

At this point, if needed, it is possible to realize the linear pattern on the bottom membrane as previously describe (chapter 2, §3.2).

2.1.4. Device preparation for the experiments

Once the cells were seeded and ready to perform the experiment the device was prepared accordingly.

Firstly, as stated before, a second slab of 1mm thick PDMS, sterilized with ethanol at 70%, was placed on top the culturing well to protect the cells from external

contamination. Since the cover is intended to be temporary, it wasn't bind with plasma activation, but it was held in place by the metal bars that were then screwed on the device to allow its insertion in the ElectroForce® planar biaxial TestBench pincers.

2.1.5. Characterization of the device deformation

As stated before, the high throughput analysis for which this device is designed, require a homogeneous deformation throughout the whole culture surface in order to be sure that the material extracted from the cell is derived from uniform conditions. The mechanical deformation of the culturing surface of device was simulated for a 10% degree of deformation, choose as a value typically used in stretching experiments to reproduce *in vivo* conditions.

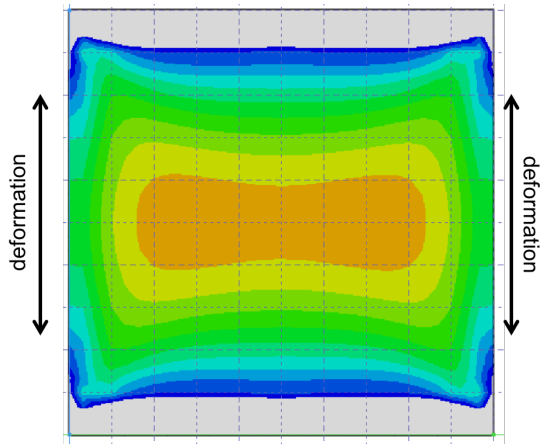

Figure 3.2.3 *Heat map of the culturing surface deformation at 10% elongation. The colored area represents deformations comprise in the interval 9-10%. The grid dimension is 2mm.*

The result of the simulation is reported in figure 3.2.3, where the deformation of the 3x3cm cell culturing area is represented as a heat map and the colored area depicts deformations in the in range 9-10%. It can be seen that the deformation pattern is quite evenly distributed along the surface, with the exclusion of two 2 mm wide stripes in proximity of the edged connected to the stretching pincers.

Overall the strain applied to the cells seems to be sufficiently homogeneous to perform the extraction analysis without risking to mix together material form cell subjected to very different levels of strain thus dampening the outcome. The areas differing more than 1% in deformation from the nominal value can be excluded during the surface functionalization, cell seeding or extraction phases to further reduce any inhomogeneity in the experiment.

2.1.6. Device sterilization and functionalization

The device was sterilized prior to cell seeding, briefly the bottom was sterilized with ethyl-alcohol at 70% concentration while the upper surface was treated with UVC for 25 minutes.

Since PDMS doesn't naturally provide any binding site for cell attachment, it is also necessary to functionalize the device surface previous to cell seeding. To this end different protocols have been used giving ultimately the same results.

In case fibronectin or laminin (Sigma-Aldrich) were used, 4.5µg of protein are needed to coat the whole device surface. The necessary amount of protein was dissolved in 3mL of PBS 1x, in order to be able to cover completely the surface with the solution and poured on the device culturing area. The solution was then left evaporating overnight and as a result the protein is left deposited on the PDMS surface. The devices are then quickly rinsed with PBS 1x to remove salt crystal and are the ready to use.

In the case matrigel was used, a solution of Reduced Factors Matrigel (Corning) at diluted in Ham F12 Nutrient Mixture (Gibco) at 2.5% was deposited on the surface an incubated for 1 hour at 37°C. Afterwards the excess solution was aspirated and the devices were ready for cell seeding.

2.1.7. "On the bench" incubator

To allow longer experiments with the mesofluidic stretching device without subject the cells to additional stress due to sub-optimal environmental conditions, an

environment control chamber made of PMMA and featuring an aluminum bottom was realized around the incubator.

A picture of the environmental control system as used during the experiments is reported in figure 3.2.4, completed with labels to pinpoint the various components of the system.

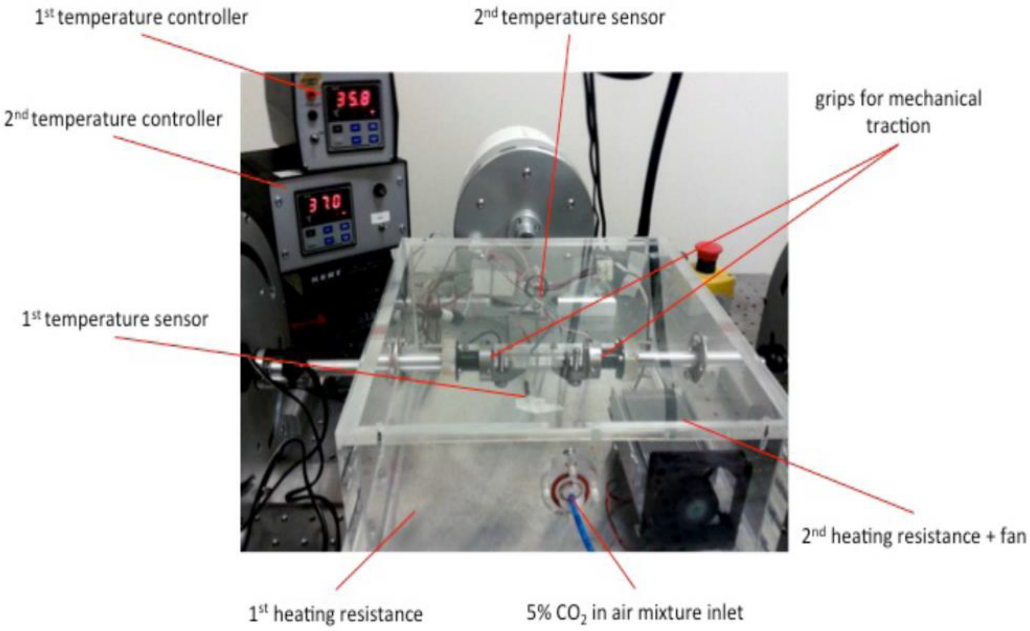

Figure 3.2.4 *Environmental control system. The developed system is composed by two temperature control loops and a gas inlet to maintain the correct CO_2 partial pressure. Humidity is guaranteed by an open petri-dish filled with distilled water.*

The main goal of the environmental control is to provide a stable temperature of 37°C for the cells during the experiment. To this end two sets of temperature control system were realized. The first one is a heavy-duty temperature control loop, entrusted with the rapid increase of temperature at the beginning of the experiments and with maintaining a stable core temperature in the environment of 36°C. It is composed by a heating resistance placed inside the aluminum base of the climate chamber, that in this way heats up the whole base, controlled by a PID temperature

controller set at 36°C. The PT100 temperature sensor is placed directly on the metallic surface.

Since the previous temperature control loop suffers from a high lag time, due to the heat capacity of the aluminum bottom, a second temperature loop was inserted to finely tune the temperature in the biological culture proximity. This controller is linked to a second heating resistance inserted in a aluminum radiator and equipped with a fan to disperse the hot air generated. The PID controller is set at 37°C and the PT100 temperature sensor is positioned as close to the cell culture as possible. The double temperature control loop ensured that the temperature oscillation at the cell culture level was maintained within the range ±0.2°C.

The CO_2 partial pressure of 5% required by cell cultures was guaranteed through a constant inlet of the desired mixture of air and CO_2 obtained through a CO_2 controller connected to the ambient air and a tank of carbon dioxide.

The last feature required to reproduce the environment of an incubator is a high level of air humidity (95%), this was accomplished by placing an open container filled with distilled water. The temperature inside the chamber favored water evaporation providing a moisturized environment.

2.2.Experiment: differentiating human myoblast

The mesofluidic stretching device along with the environmental control system were tested analyzing the response to mechanical stretch of differentiating human myoblast (muscle fibers), in collaboration with prof. Giorgio Valle from the University of Padua.

These experiments were necessary to validate the biological integration in the developed culturing device, and especially to verify whether short term exposure to mechanical strain is able to trigger a biological response.

The aim of this collaboration was to gain further knowledge in the molecular mechanisms that drive skeletal muscle response to mechanical *stimuli* analyzing the changes in the transcriptome through Next Generation Sequencing (NGS).

For these experiments the cells were forced to align through creating a linear pattern following the physical PDMS patterning protocol described in chapter 2, §3.2, in order to better reproduce the *in vivo* environment of muscle fibers

2.2.1. Experimental plan

Human primary myoblast cells CHQ5B were seeded in laminin-treated mesofluidic devices and cultured in Dulbecco's Modified Eagle's Medium (DMEM, Gibco) supplemented with 20% Fetal Bovine Serum (FBS, Thermofisher Scientific) and 100µg/ml gentamycin. When cell density was suitable, the cell culture was placed in serum starvation using DMEM supplemented with 2% Horse Serum (HS, Thermofisher Scientific) to promote cell differentiation into myotubes.

24 hours after the beginning of the differentiation protocol, cells were stretched for 30 minutes at 0.2 Hz and 10% elongation, the mechanical strain was uniaxial parallel to cell orientation.

Immediately after the stretching experiment the culture medium was changed and cells were kept in differentiating culture for 3 or 40 hours to study respectively the short and long term biological response. At the selected time points, the RNA was extracted to perform the NGS analysis both from the mechanically stimulated cells and from their respective static controls.

2.2.2. Results and discussion

The analysis was performed analyzing the differentially expressed genes at the three and forty hours time points comparing the stimulated cells and the corresponding controls. A gene was considered differentially expressed if the relative difference was at least ±1.4 times.

In figure 2.3.5 the results obtained are reported both as scatter plots for the 3 hours post stretch (2.3.5a), 40 hours post stretch (2.3.5b) and comparison between 3 and 40 hours post stretch (2.3.5c) and as a bar plot that summarizes the findings (2.3.5d).

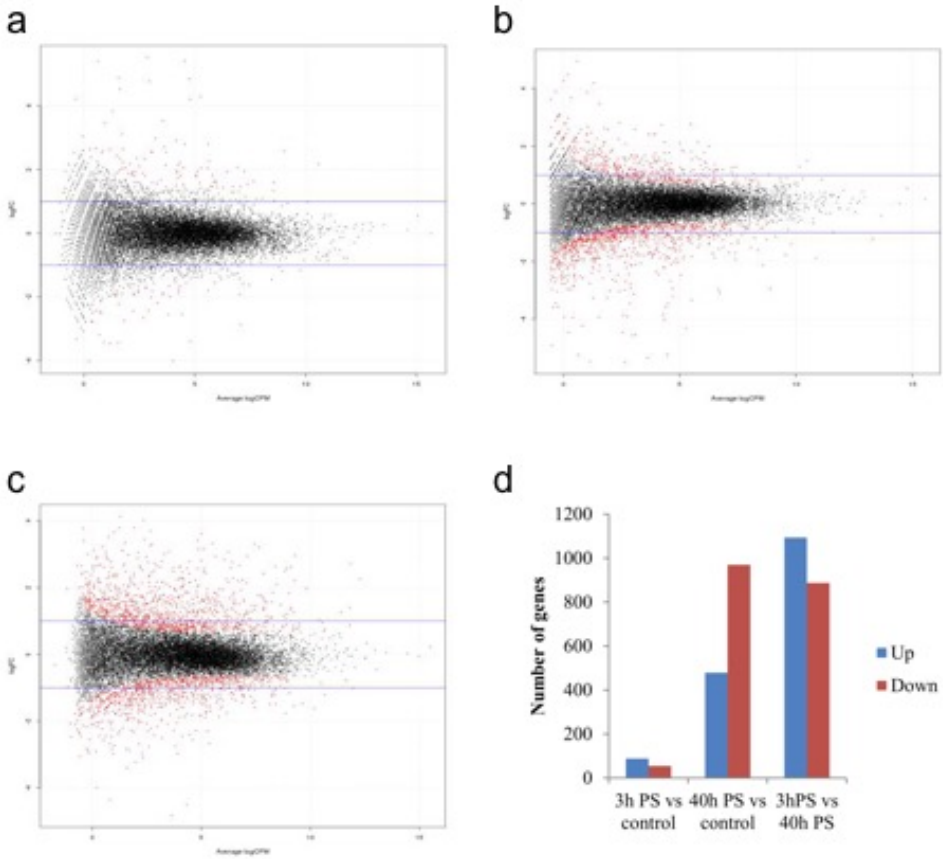

Figure 2.3.5 *Results of the NGS. Scatter plot of differentially expressed genes at 3 hours post stretch between stimulated and control cells (a), scatter plot of differentially expressed genes at 40 hours post stretch between stimulated and control cells (b), scatter plot of differentially expressed genes in the stretched cells between the two time points (c) and bar plot of the findings (d).*

At the three hours time point, the number of differentially expressed genes between stretched ad controls cells is 142, suggesting that the mechanical strained was sensed by the cells and it ensued a biological response.

At the forty hours time point the number of differentially expressed genes is one order of magnitude higher than before, showing a total of 1447 affected genes, indicating that the biological response to short term stimulation is quite stable in time and, once activated, its effects propagate over long period of time probably through the involvement of several signaling pathways characterized by different time spans.

A comparison between cells at the two time points was also performed, in figure 2.3.5c and d, such analysis for the stimulated cells is reported. It can be seen that in this case the number of differentially expressed genes is higher respect to the other comparisons performed. This is to be expected since the cells are actually undergoing differentiation and, as a result, specific genes are turn on and off during the progress of the differentiation. However, it is interesting to note that the difference in the transcriptome is much higher in the case of the cells that underwent mechanical stimulation with respect to the control counterparts, as reported in figure 2.3.6.

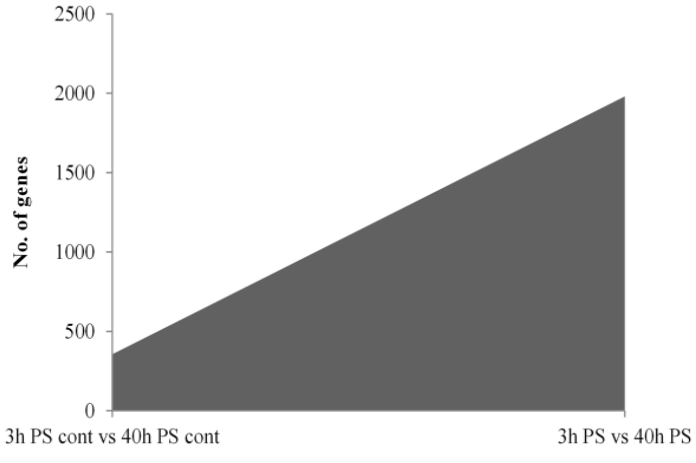

Figure 2.3.6 *Comparison between the number of differentially expresses gene between 3 and 40 hours post experiment for the control cells (left) and the stimulated cells (right).*

The difference in the transcriptome profiles between stimulated and controls cells is an indicator that a biological adaptation to mechanical stress is underway, to gain further insight on the biological functions affected by this changes, a search for enriched GO terms and a pathways analysis using KEGG database were performed.

In the short term response to mechanical strain, 3 hours after the stimulation is imposed, mainly genes involved in the immunogenic response are triggered, as indicated by the up regulation of genes related to immune and wound response, cell proliferation and taxis and chemotaxis. The pathways analysis, reported in figure

2.3.6a, shows an increase in intracellular signaling (cytokine-cytokine receptor interaction) and the activation of intercellular signaling pathways such us TNF and chemokine signaling pathways.

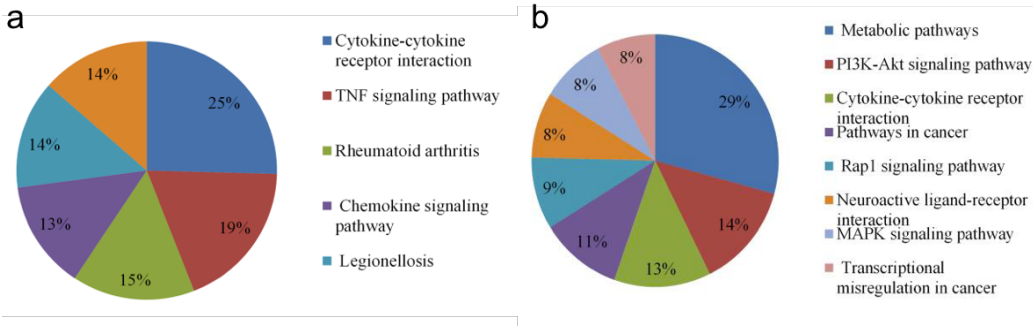

Figure 2.3.6 *KEGG pathways analysis of the genes differentially expressed between controls and stimulated cells at three hours post-stretching (a) and forty hours post stretching (b).*

In the long term response, 40 hours after the mechanical stimulation is applied, mainly metabolic pathways were up regulated, as indicated also by the pathways analysis whose findings are reported in figure 2.3.6b, along with genes related to the responses to nutrient levels and insulin *stimulus,* on the other hand, genes up regulated at the earlier stage, appeared to be down regulated in the 40 hours time point.

Interestingly, some genes up regulated in the short term response to stretch are the same ones involved in later stages of muscular differentiation and in the long term response many genes of the myosin family were also up-regulated, so it appears like mechanical strain hastens some molecular features of muscle differentiation.

Summarizing the results obtained from this experiment, the short term response of mechanically stimulated cells is mostly a transient inflammatory and immunogenic response, as mechanical strain is immediately perceived by cells as an injury. At the same time the muscle growth process appears to be enhanced through the early activation of differentiation-driving genes and also cell metabolism seems to be affected by mechanical strain.

3. Microfluidic stretching device

The microfluidic stretching devices has been developed to perform prolonged stretching experiments of cultured cells since it can work inside an incubator. On the other hand, the reduced culturing area and, even more so, the fact that not all culturing area is actively stretched limit the biological assays that can be used, ruling out the techniques that require high initial amount of material such as DNA, RNA and protein quantification.

Even though, if necessary, this limitation can be overcome by selectively extracting cell just from the stretched areas and by pooling together samples from several devices, the principal biological assay that will be conducted using these devices is immunofluorescence staining, taking advantage of the full optical compatibility offered by microfluidic devices.

In the following paragraphs firstly the materials and methods used to realize the microfluidic stretching devices will be described, then the experiments performed using this technology will be presented and the results obtained will be discussed.

3.1. Materials and methods

The microfluidic stretching device was developed using standard soft-lithography and replica molding techniques as described in the following sub-paragraphs.

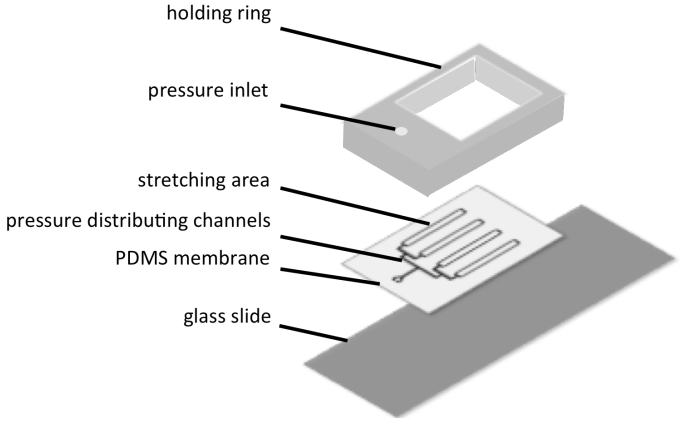

Figure 3.3.1. *Representation of the microfluidic stretching device highlighting the three constitutive layers: glass slide, PDMS membrane with engraved inflating system to provide stretching and holding ring.*

The device is composed of three layers as schematized in figure 3.3.1: the bottom layer is made of glass slide that provides mechanical support, attached to the glass there is a thin PDMS membrane in which a system of inflatable areas is impressed *via* soft-lithography and that provides the actual mechanical stress and finally a holding ring is attached on topo of the membrane to create a culturing well and allow the connection of the pneumatic inlet necessary for membrane inflation.

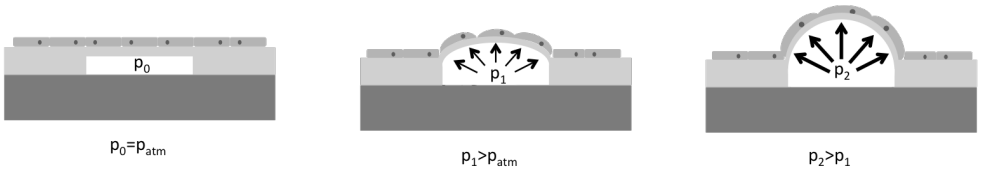

Figure 3.3.2. *Schematization of the working principle. The cells adhere to the PDMS surface, when the system is at rest (p_0) the cells are not stretched. When the pressure inside the inflating channel is increased (p_1) the elastomeric membrane inflates and thus stretches the cells seed on top of it. If the pressure is further increased (p_2) the achieved stretching is greater.*

The mechanical stretch is achieved in the stretching areas by inflating the thin elastomeric membrane through pressure increase, modulating the pressure built up allows to determine the percentage of strain transmitted to the cells (figure 3.3.2)

3.1.1. Mask design

The design of the inflating areas and the pressure distribution system was realized in AutoCAD 2D (Autodesk) setting the measurement units in microns and the length accuracy up to the fourth decimal, moreover to avoid tensional points all angles have been rounded off, the final design is illustrated in figure 3.3.3. The design was later exported to Adobe Illustrator (Adobe) to blacken all the areas of the photomask that must prevent UV radiation, which in this case comprises everything but the inflating

areas and the pressure distribution channels. The design was then printed at 8000dpi on photographic film to obtain the photomask.

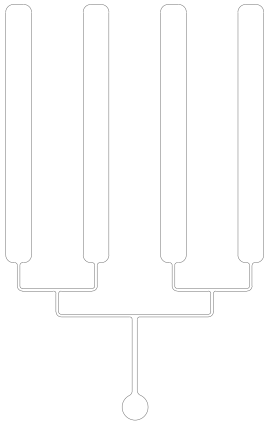

Figure 3.3.3. *Mask design of the microfluidic stretching system. The rectangles are the active stretching areas, connected to a single inlet by a system of specular pressure distribution channels.*

The stretching areas were designed as rectangles 1mm wide and 10mm long, this geometrical configuration was chosen to allow the study of the mechanical response of cellular couplings. Indeed, by creating a linear pattern perpendicular to the main strain, as described in §1.3, the cells will align accordingly and the cellular junctions will be explicitly stressed.

The area between two stretching rectangles was set to be 2mm in order to guarantee correct adhesion of the elastomeric membrane.

The pressure delivery system was designed as to have the same pressure drop in all branches in order to obtain an even pressure difference, and thus mechanical stretch, among the separate stretching areas.

The whole design, including the outer holding ring, fits in a standard microscopy slide 25mm wide.

3.1.2. Mold fabrication

The membrane with engraved stretching areas and pressure distributing channels was produce *via* replica molding, so the mold needed to be produced using standard soft-

lithography techniques. Untreated silicon wafer of 4" diameter (Siegert Wafer) were used, fitting eight stretching devices in a single wafer.

The wafer was cleaned with methanol and ethanol to remove any surface contamination and finally rinsed with MilliQ water and dried on a hotplate set a 115°C. The wafer was then centered in the spin coater (Laurell) and negative SU8-2050 photoresist (Microchem) was poured on the center until about one third of the surface was covered. The resist was left resting for a minute before starting the spinning program to allow relaxation of the polymer and avoid possible defects in the spinned layer.

The spinning program used was as suggested by the manufacturer manual to achieve a final thickness of 40µm, briefly a two step program was followed:

Time (s)	**Speed (rpm)**	**Acceleration (rpm/s)**
10	500	100
30	4000	300

Subsequently the wafer was set on a levelled plane for 5 minutes to reduce residual stress in the resist in order to avoid defects in the resist layer and to reduce the edge effect, and then it was placed on a levelled hot plate (Falc) at 95°C for 6 minutes as specified by the manufacturer's manual to allow the evaporation of the solvent.

Following, the wafer was ready for UV exposure. Using a negative type photoresist the UV radiation cures the resist thus the resist is polymerized only in the exposed areas of the photomask. Prior to exposure, the UV lamp (OAI Lamp) energy intensity was checked in order to determine the exposure time necessary to reach the energy flux specified by the manufacturer's manual which equals 160 mJ/cm^2. The resist was then exposed through the photomask for the required time and afterwards was placed on the levelled hot plate at 95°C for another 6 minutes.

At this point it is possible to develop the mold. The wafer was placed in a bath of methossimethacrilate (Sigma-Aldrich) and gently stirred for 10 minutes, afterwards it

was rinsed with isopropanol which blocks the dissolving action of methossimethacrilate and moreover reacts with the uncured resist forming a milky residue and indicating when all the uncured resist is removed. In the presence of milky residues, the wafer was placed back in the methossimethacrilate bath for another couple of minutes and then the process was repeated until all the uncured resist was removed. At this point the wafer was washed with isopropanol and dried with a flux of nitrogen and the mold was completed and ready for use.

3.1.3. Replica molding

Replica molding was used to obtain the PDMS membrane with the stretching areas and pressure distributing channels engraved. To this end the mold was firstly silanized with hexamethydisiloxane, HMDS, (Sigma-Aldrich) to promote the detachment of the silicone membrane after curing, this was accomplished placing the wafer in a vacuum container at 10^{-2}mbar for 30 minutes with a drop of silane. The low pressure causes the HMDS to evaporate and then to be evenly distributed on the wafer surface.

In the mean time the PDMS prepolymer was prepared mixing Sylgard 184 base and curing agent in a 10:1 weight ratio and degassing extensively the mixture in a vacuum chamber. Once the wafer surface treatment was completed, 4g of the prepolymer were poured on the mold and again placed in a vacuum chamber to remove all air bubbles that may cause defects in the final membrane. The wafer was then spinned firstly at 300 rpm, acceleration 100 rpm/s for 30 s to evenly distribute the prepolymer on the surface and then at 700 rpm, acceleration 100 rpm/s for 60 s to obtain a final thickness of 70µm as determined previously in the laboratory (figure 3.3.4, Michelin 2009).

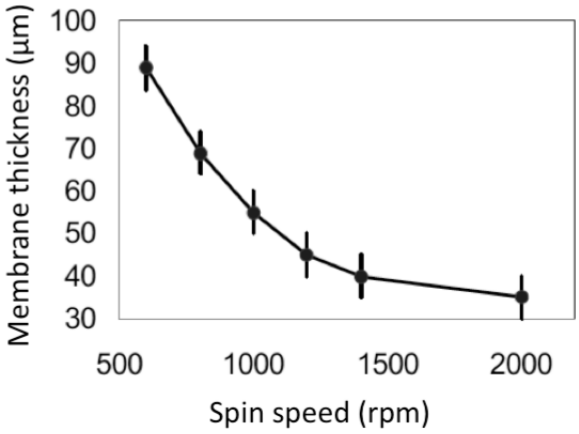

Figure 3.3.4 Membrane thickness versus final spin speed for 10:1 weight base to curing agent ratio PDMS (Adapted from Michielin 2009).

The PDMS was then cured at 80°C for 1 hour on a levelled hotplate. After curing is completed the PDMS membrane can be extracted from the wafer and the mold can be reused.

3.1.4. Microfluidic chip fabrication

As shown in figure 3.3.1, the microfluidic chip is composed of three layers, a glass slide, the PDMS membrane and the holding ring, the three layers were prepared separately and then assembled together.

Prior to use the glass slides were washed with low foam soap and dried with a flux of nitrogen.

The PDMS membrane with engraved stretching areas and pressure distribution channels production was described in the previous paragraph (§3.1.3).

The holding ring was obtained by a block of PDMS prepared with a 10:1 weight ratio of base and curing agent, approximately 3mm thick and cut with a scalpel to obtain the required shape.

To assemble the microfluidic device firstly the holding ring was bounded to the membrane still attached to the wafer mold *via* plasma surface activation. Briefly the two surfaces that needed to be bind together were placed in a plasma cleaner (Herrick

Plasma) facing upwards. The plasma cleaner chamber was sealed and the pressure was reduced to $3*10^{-1}$mbar, then the plasma was switched on and left active for 2 minutes. Afterwards the pressure in the chamber was restored and the holding ring and the wafer were extracted, the holding ring was then pressed on the PDMS carefully avoiding to trap air between the two surfaces. The two pieces were briefly placed on a hot plate at 50°C to promote adhesion, then the membrane was cut with a scalpel following the shape of the holding ring and finally it was possible to extract the membrane, attached to the ring, form the mold.

The microfluidic device was completed attaching the glass slide through plasma surface activation operating as describe previously. Before bounding the silicone layers to the glass, the inlet of the pressure distributing channels was realized in the holding ring using a 1mm diameter punch.

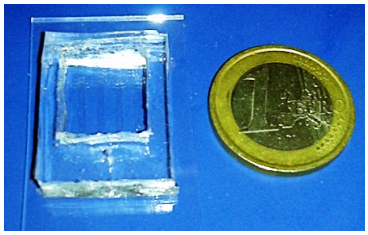

Figure 3.3.5 *Picture of the microfluidic stretching device.*

Once assembled, the device was left on a hot plate at 80°C for 2 hours to promote the adhesion between the layers. Prior to use all devices were tested connecting them to a syringe and verifying that all the stretching areas were able to inflate and that the membrane remained adherent to the glass slide and didn't brake when pressure was increased.

In figure 3.3.5 a picture of the completed device is reported. The three layers can still be recognized and the overall size is determined by the glass slides used as support, typically rectangular slides of 24x40 mm.

3.1.5. Device sterilization and functionalization

The microfluidic device needed to be sterilized prior to cell culturing. The bottom and outer parts of the devices were sterilized dipping them quickly in ethanol at 70%$_{vol}$ concentration. The culturing well instead was sterilized through exposure to UVC for 25 minutes.

Prior to use the devices culturing surface had to be treated with a suitable protein coating to allow cell adhesion since PDMS doesn't provide any anchoring point for cells. The functionalization was performed with Matrigel (Corning), a gelatinous protein mix derived from secretion of mouse sarcoma cells, briefly 500µl of 2.5% Reduced Factor Matrigel diluted in Ham F12 Nutrient Mixture (Gibco) was poured on the device surface in order to cover it completely and left incubating for at least 1 hour, prior to cell seeding the excess solution was discarded.

3.1.6. Experimental set up and calibration

In order to enforce cyclic stretching, the microfluidic stretching device has to be connected to sources of different pressure. As schematized in figure 3.3.6, the high pressure reservoir consisted in an air compressor (Porter-Cable), equipped with a 1.5L tank. The pressure in the tank was kept between 10bar and 8bar and the outlet was regulated by a coarse embedded pressure regulator, set at about 1 bar. The pressurized air then flowed through a sterilizing filter of 22µm diameter pores (Millipore) to protect the downstream equipment from dirt and the pressure was tuned to the value determined to obtained the required deformation by a second fine pressure regulator (CKD). The frequency of cyclic stretch during this experiments was set at 1hz, so the low pressure used was ambient pressure, if higher frequencies are required the system needs to be connected to a vacuum chamber.

Both pressure sources are connected to a computer-controlled three-way valve, and the outlet is connected to the stretching devices directly inside the incubator; through a custom generated script (Michielin *et al.* 2015) it is possible to select which

inlet is opened thus obtaining the cyclic deformation.

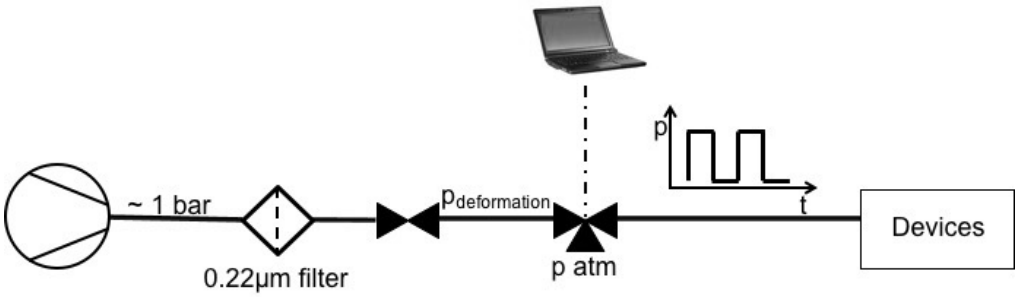

Figure 3.3.6 *Schematization of the experimental set up for the microfluidic stretching devices. The devices are connected to a computer-controlled three-way valve whose inlets are the low pressure reservoir, in this case ambient pressure, and the high pressure reservoir, in this case an air compressor.*

Prior to use the system was calibrated to determine the pressure ($p_{deformation}$) required to obtain a given deformation of the PDMS membrane and thus of the cells attached to it.

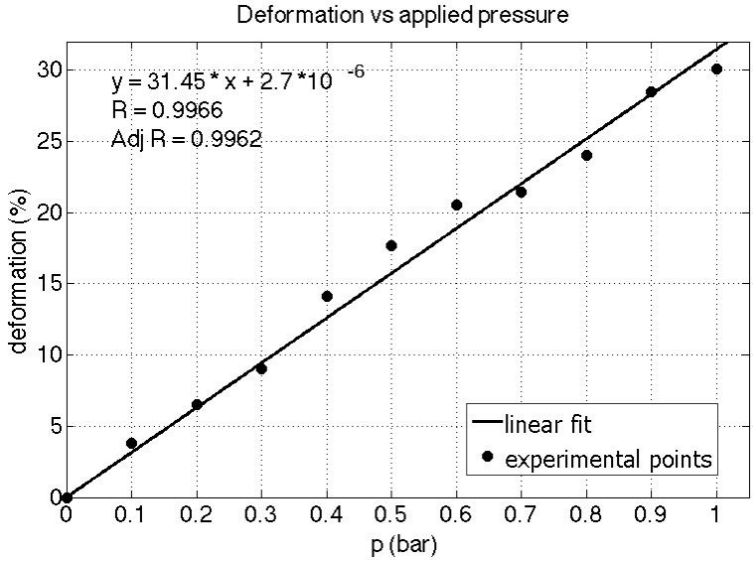

Figure 3.3.7 *Calibration of the stretching system. The deformation at different applied pressure was measured and plotted (experimental points) and a linear fit was obtained using MATLAB regression suit.*

To this end the membrane was marked and the applied pressure was increased

stepwise by 0.1 bar, each time the stained area was recorded and measured to determine the achieved deformation. The experimental points were then uploaded in Matlab (Mathworks) and, using the Curve Fitting Tool, a linear fit was calculated. As shown in the graph in figure 3.3.7, the selection of a linear fit is justified by the trend of the experimental points, and consequently the fit obtained is very good as confirmed by R = 0.9966.

Using this calibration curve it is now possible to determine the pressure required to achieve the desired deformation, the correlation was calculated for applied pressure up to 1 bar so it shouldn't be used for higher values. Anyways at 1 bar the corresponding deformation is 30%, a value sufficiently high to replicate both physiological and pathological strain conditions found *in vivo*.

3.2. Experiment: differentiating Vascular Smooth Muscle Cells

The microfluidic stretching device was used to study the role of mechanotransduction during the development of the cardiovascular system and the effect of aging in this context. These experiments resulted from a collaboration between Prof. Elvassore and Prof. Belmonte and were carried out in the latter laboratory of Gene Expression at the Salk Institute for Biological Studies in La Jolla, California, USA.

The aim of this joint project was to study the role played by mechanotransduction and mechanical stress during the differentiation of stem cells into vascular smooth. Since differentiation essentially recapitulates embryogenesis this study will help unravel the pathways that lead to the correct development of the cardiovascular system and, also, will give an insight on the biological mechanism that allows the recruitment of progenitor cells for wound healing in the adult organism.

Moreover, since one of the major risk factors connected to vascular system diseases and morbidity is aging, both healthy and senescent cells behavior was investigated and compared in order to discover which pathways are affected during aging resulting in the diminished ability to recover damage.

3.2.1. Biological models

These experiments were performed using four different cellular models. Firstly, to establish the wild-type response of differentiating vascular smooth muscle cells, H9 cells, a commercially available line of human Embryonic Stem Cells (hESCs), were used. To analyze the effect of a senescent environment in the biological response to mechanical strain two different models of accelerated aging were used, of which human induced Pluripotent Stem Cells (hiPSCs) derived form patients were already available in the laboratory (Liu G.-H. *et al.* 2011a and Zhang W. *et al.* 2015).

The first model employed was Hutchison-Gilford Progeria Syndrome (HGPS), the most severe cellular model of premature aging. Hutchison-Gilford Progeria Syndrome is a rare autosomal dominant premature aging syndrome most frequently caused by a *de novo* mutation in the LMNA gene which encodes proteins called lamin A and C, involved in the nuclear intermediate filament. The mutation causes the transcription of a truncated form of prelamin A that cannot be correctly processed into mature lamin A and thus result in the accumulation of a farnesylated intermediate called progerin (Verstraeten *et al.* 2008) that in turn leads to abnormal nuclear shape ad compromised nuclear integrity (Dhal *et al* 2006, Scaffidi and Misteli 2005).

Patients affected by Hutchison-Gilford Progeria Syndrome commonly die in their teens (Pollex *et al.* 2004) most frequently (>90%) due to myocardial infarction or stroke resulting from progressive arteriosclerotic disease (Verstraeten *et al.* 2008).

Durning the experiments also hiPSCs derived from Hutchison-Gilford Progeria Syndrome patients carrying a gene correction to restore a healthy phenotype (cHGPS) were available (Liu G.-H. *et al* 2011b) and were employed as isogenic controls of the HGPS cells.

The second model of premature aging was Werner Syndrome, an autosomal recessive disorder in most cases caused by mutations on the WRN gene, a member of the RECQ helicase gene family responsible for stable genome maintenance (Shimamoto *et al.*

2015, Cheung *et al.* 2015). Accelerated aging due to malfunctioning of WRN is generally related to its role in DNA repair and replication and in telomeres maintenance, as age progresses the DNA damage is accumulated resulting in cellular senescence, apoptosis, cell cycle arrest or accelerated telomeres loss and eventually reaches a pathogenic threshold leading to the onset of age-associated diseases and predisposition to cancer (Pichierri *et al.* 2011, Shimamoto *et al.* 2015).

These two different models of aging were chosen because they were readily available and largely investigated in the scientific literature (Cheung *et al.* 2015), but more importantly because the pathological onset of this two diseases is caused by different biochemical pathways, thus a similar response to mechanical stress compared to that of healthy control could be an indicator of a senescent behavior not determined by the specific pathology.

3.2.2. Stem cells cultures and vascular progenitors cells derivation

The four lines selected for the experiments had to be maintained and expanded before use. Moreover, it was verified that stem cells couldn't be directly used for the mechanotransduction experiments since they detached from the substrates by two days after the onset of mechanical stress. To overcome this problem, before starting the stretching experiments, the cells were pre-differentiated into angioblast-like progenitors with the potential to further differentiate into vascular lineages (Kurian *et al*. 2013).

For what concerns maintenance and expansion of stem cells the well established technique for feeder-free culture was used (Amit *et al.* 2004).

Briefly, the stem cells were cultured in standard 6-well multiwells (BD), prior to seeding the wells were treated with Matrigel (Corning) to promote cell adhesion placing 2 mL of Reduced Factor Matrigel diluted in Ham F12 Nutrient Mixture (Gibco) at 1mg/mL concentration and leaving the solution in a incubator at 37°C for at least 2 hours to allow the Matrigel to jellify and aspirating the excess solution before cells

seeding. Stem cells were cultured using a specific culture medium suitable to maintain the undifferentiated state directly purchased from the Salk Institute Stem Cell Core, the medium was changed once every 24 hours. When the medium was changed the stem cells colonies were visually inspected and all areas of spontaneous differentiation were manually removed to maintain the pluripotent state of the culture. Once 75% confluence was reached the cells were passaged using a 1:3 or 1:6 splitting ratio. To this end the spent medium was discarded and the cells were washed with Ham F12 Nutrient Mixture (Gibco) and then were treated with Dispase (StemCell Technologies), a protease suitable for gentle dissociation preferred over other proteases such as trypsin since it detaches the stem cell colonies from the culture plastic but doesn't disaggregate them. The cells were incubated at 37°C with Dispase for 5-7 minutes or until the stem cell colonies edges began to curl up, then the protease was aspirated and the cells were washed thrice with Ham F12 Nutrient Mixture (Gibco). After completing the washing, an exact quantity of culturing medium varying between 1 to 2 mL depending on the desired splitting ratio was added and the cells were gently scraped from the well surface using a glass pipette. The suspension of cells was then distributed in the new wells according to the desired splitting ratio.

As stated before, the stem cells were differentiated in angioblast-like vascular progenitors cells before they could be employed in the stretching devices. For the differentiation the stem cells were split in 6-well multiwells using a splitting ratio of 1:10 to ensure that by the end of the differentiation protocol the culture isn't over-confluent, and were cultured for ten days with Mesoderm Induction Medium (MIM), developed in the hosting laboratory (Kurian *et al.* 2013), changing the medium once every other day. In the published paper it is reported that 8 days are sufficient to achieve the mesodermal commitment, however it was verified that prolonging the mesodermal induction culturing conditions until day 10 increased the percentage of angioblast-like cells to almost 100%, eliminating the need to sort cells before starting

the experiments.

3.2.3. Cell seeding in the microfluidic devices

The vascular progenitor cells obtained as described previously were washed with PBS and then treated with TrypLE Express (Invitrogen) to promote their detachment from the culturing well. When all the cells were detached, the suspension was collected and centrifuged at 1400 rpm for 5 minutes to separate the cell pellet from the supernatant. The cells were then suspended in an exact volume of MIM and seeded in the devices, previously coated with Matrigel as described in §3.1.5, using a 1:5 splitting ratio, since the device surface area is roughly ¼ of the surface area of a 6-well well, every well of mesodermal progenitors was split into 20 devices.

For each experiment a total of 21 devices were seeded, nine devices to perform the stretching experiments and twelve to provide the static controls, three of which were used as negative controls in the following analysis. Moreover, the cells were seeded also in 6-well multiwells as an internal reference to compare the results obtained during this experiments with previous work performed in the laboratory using standard culturing conditions.

3.2.4. Stretching experiments

After seeding the devices were kept in static conditions for 24h hours to allow the cells to properly adhere to the surface, afterwards the medium was switched to Smooth Muscle Growth Medium 2, SmGM2 (Lonza), then the devices were connected to the pneumatic system and the mechanical stimulation was started on the 9 actively solicited devices.

The mechanical strain was set to be 10% elongation, corresponding to a deformation pressure of 0.3bar, at 1HZ to mimic *in vivo* conditions (Chen *et al.* 2003). The experiments were conducted stretching continuously the cells and changing the medium once every other day. Time points were selected at 6, 8 and 12 days after the beginning of the differentiation protocol into Vascular Smooth Muscle cells and the

beginning of the mechanical stimulation. This time points were selected to check an early response of the cells (time point six days) and the response at the fulfillment of the differentiation protocol (time points eight and twelve days), as it was previously tested that the percentage of vascular smooth muscle cells didn't significantly increase after twelve days.

3.2.5. Analysis

The cellular response to mechanical strain was probed analyzing the percentage of cells differentiated into vascular smooth muscle, to determine if a cell was differentiated an immunofluorescence staining against calponin was performed. Calponin is a troponin T-like protein that binds to actin filaments expressed by contractile smooth muscle cells, hence it is widely accepted as a marker of differentiated smooth muscle cells (El-Mezgueldi 1996).

At the selected time points three stretched devices and four static controls were randomly selected, rinsed with PBS 1x (GIBCO) and fixed with paraformaldehyde, PFA, (Sigma-Aldrich) at 4% concentration for 10 minutes. The devices were then washed thrice with PBS 1x for 5 minutes each to strip away all residual PFA, and then were treated for 8 minutes with PBS 1x supplemented with 0.1% of Triton X-100 (Sigma-Aldrich) to permeabilize the cellular membrane. After the permeabilization the cells were rinsed with PBS 1x and then treated for 45 minutes with PBS supplemented with 1% of heat inactivated Horse Serum (StemCell Technologies), a solution known as blocking solution. After completing the blocking, the sample are washed with PBS 1x and ready for the immunofluorescence staining.

Firstly, the primary antibody against calponin (Daco M3556, anti-human in mouse) was incubated for one hour at room temperature, briefly a 40µl drop of a solution of antibody diluted 1:50 in blocking solution was pipetted on the sample surface and covered with a piece of parafilm to distribute it evenly throughout the whole surface. After the incubation was completed the sample was washed three times for 5 minutes

each with PBS 1x to remove all the unreacted antibody. Every time, one of the static devices was used to check the specificity of the secondary antibody, that is to check if the secondary antibody, which is the fluorescent probe, reacts and links only with the primary antibody or not; in this case the primary incubation was carried out as before but using just the blocking solution.

Finally, the fluorescent probes were incubated, this includes the secondary antibody for staining calponin, for which an anti-mouse green emitting fluorophore was selected, and Hoechst 33342 (Thermofisher Scientific), a fluorescent dye emitting in blue that links to eukaryotic cells DNA, thus marking the cells' *nuclei*. Both dyes were mixed together in the blocking solution respectively at a 1:300 ratio for the secondary antibody and 1:500 for the Hoechst dye. As before, a 40µl drop was deposited on the surface and spread evenly with the aid of parafilm.

The secondary incubation was carried out at room temperature for one hour and afterwards the samples were washed thrice with PBS 1x and finally stored at 4°C in PBS 1x supplemented with 1% Penicillin-Streptomycin until analyzed using an Olympus 1X51 upright fluorescent microscope (Olympus).

3.2.6. Results

The fluorescent-stained samples were analyzed at the microscope taking pictures of randomly selected areas at 20x magnification for bright field and both the fluorescent probes used. The pictures were merged using ImageJ and the percentage of calponin positive cells, which corresponds to terminally differentiated vascular smooth muscle cells, was calculated, in figure 3.3.8 an example of the data thus obtained is reported. In the case of the stretching devices, the distinction between actively stretch areas and non stretched areas was maintained during the analysis.

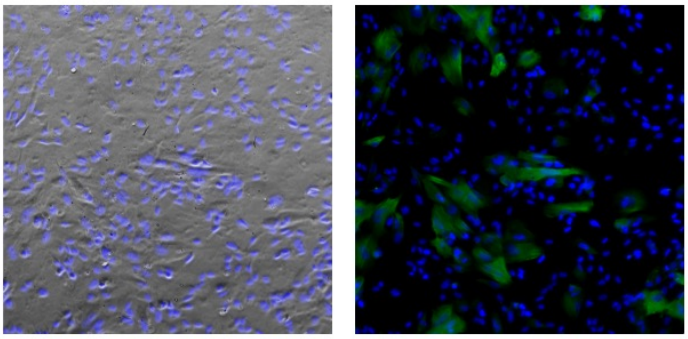

Figure 3.3.8 *Example of the staining. On the left is reported the merge between bright field and Hoechst staining the nuclei (blue), on the right the merge between Hoechst (blue) and calponin (green).*

Firstly, the cell morphology was inspected. It has been previously reported (Chen *et al.* 2003, Standley *et al.* 2002, Li *et al.* 2003) that cells sensing mechanical stress re-orient aligning perpendicularly to the main axis of strain to reduce the cell deformation. Therefore, also during this experiments the alignment of cells subjected to mechanical strain was analyzed.

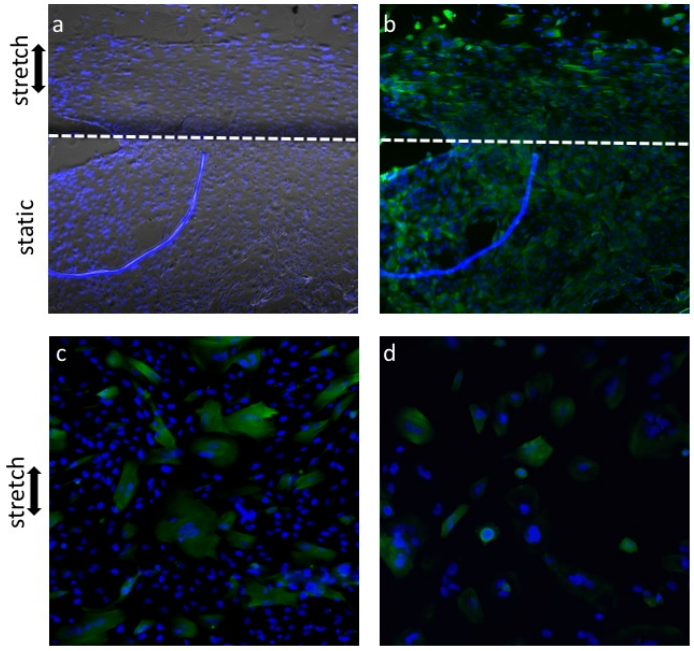

Figure 3.3.9 *Cells subjected to mechanical stress align in a direction perpendicular to the strain axis (a and b; cHGPS at day 12). However if the initial seeding density was to high cells failed to align (c; H9 at day 6). In the case of progeria cells the alignment was never observed (d, HGPS at day 6).*

As shown in figure 3.3.9a-b, also during this experiment healthy cells tended to align perpendicularly to the main axis of stimulation as expected. It was noted however that, if the initial seeding density was to high, cells failed to show a preferential alignment, probably because the high density hindered cells motility (figure 3.3.9c). On the other hand, cell alignment was always lacking in the case of progeria cells, suggesting an impaired mechanical sensing within the cells (figure 3.3.9d).

The inspection of cell morphology in response to mechanical strain gave a preliminary indication that the senescent niche interferes with the correct sensing and response to mechanical strain, to further investigate this effect the differentiation in Vascular Smooth Muscle Cells was studied.

For each cell line and time-point three samples were analyzed, averaging their results and calculating the standard deviation. Moreover, the comparison between different experiments was performed using the standard Student T test using the function embedded in Excell (Microsoft) to evaluate the statistical significance of the results.

For ease of comparison between the different cell lines, the percentage of calponin positive cells in the stretched devices was normalized to that obtained in the relative static control. In this way, potential differences absolute number of differentiated cells due intrinsic feature of the cell line are erased highlighting the effect of mechanical stress.

In figure 3.3.10 the results obtained comparing the actively stretched areas with the static controls are reported for whole four cell lines studied at the three time-points considered.

At day six both H9 and cHGPS cells lines show a strong cellular response to mechanical strain, as indicated by the average 4-fold increase of differentiate cells in the actively stretched areas compared to the static controls. The HGPS cells show no response to mechanical strain, as was expected considering the impairment of mechanical

coupling between the chromatin and the cytoskeleton due to the incorrect maturation of lamin A. WS cells show a mitigated response to mechanical cues, but the increase on differentiated cells is halved respect to the healthy cells lines.

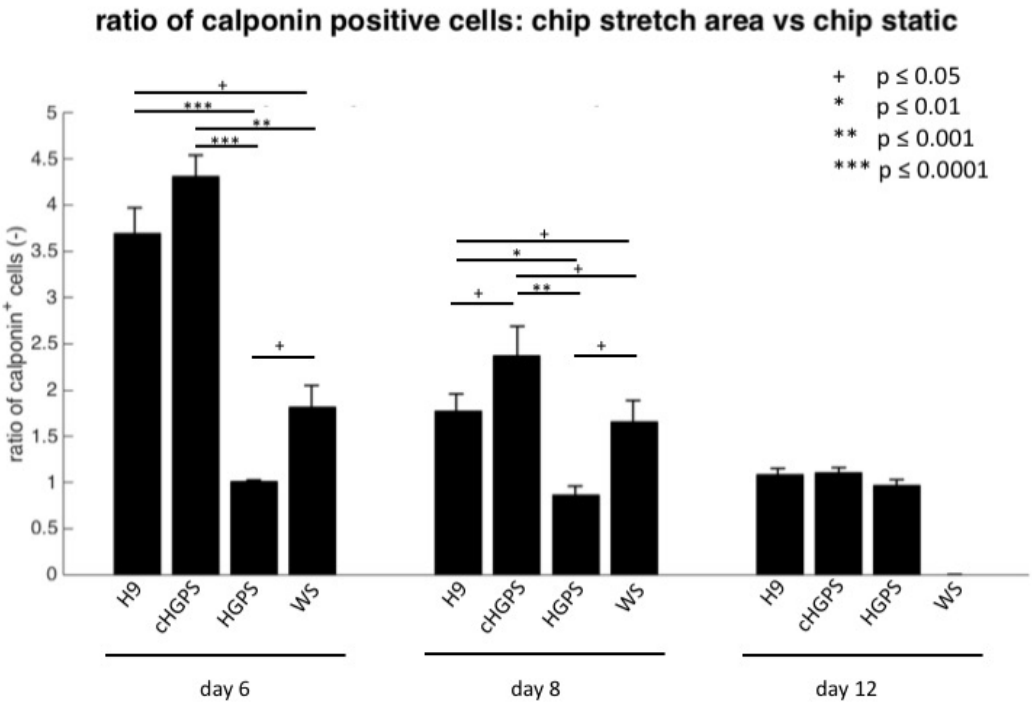

Figure 3.3.10 *Number of calponin positive cells in the actively stretched areas normalized respect to the number of calponin positive cells in the static controls. The error bars represent the standard deviation calculated on three samples.*

At day eight the number of terminally differentiated vascular smooth muscle cells in the stimulated samples is still higher compared to the corresponding static controls, but the difference is greatly reduced respect to the earlier time point. Moreover, the number of cells in the stretched devices of the senescence biological models appeared to be lower to that of their static controls, while no difference was detected in the healthy lines, however it was not investigated whether this difference was due to lower proliferation rate or higher apoptosis rate, or a combination of the two factors, in the senescent cells.

At day twelve no statistically significant difference in the number of differentiated cells can be observed between static and stretched cells, indicating that mechanical strain increases the rate of differentiation in the cells able to sense and response to the external cue, but doesn't affect the final percentage of differentiation, which for all cell lines was about 80%. Interestingly, at this time point all WS cultured in the mechanically stretched devices detached from the substrate, this is why there's no data reported for WS at this time point, the cells in the static controls on the other hand appeared to grow normally as can be seen in figure 3.3.11.

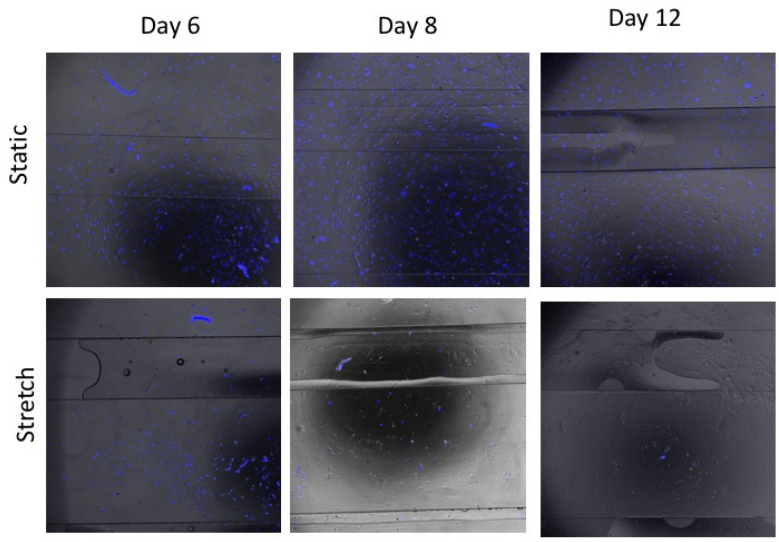

Figure 3.3.11 *Number of WS cells in the static and stretched devices at different time-points. It can be seen that the number of cells, marked by the nuclei stained in blue by Hoechst, in the static device grows in time until confluence is reached, while in the actively stretched devices the cells die and detach from the substrate.*

The same analysis was performed comparing the behavior of cells cultured in the stretched devices, but not in the actively stretched areas, with that of the cells in the static controls, as shown in figure 3.3.12. It is interesting to note that the trend observed in figure 3.3.10 still applies, though in this case the differences between stimulated cells and controls, when present, are lower with respect to the actively

stretched areas.

This result suggests that the behavior of cells seeded in the non-actively stretched areas of the mechanically stimulated devices is closer to that of the stretched cells rather than the one of the non-stimulated cells, probably due to the activation of inter-cellular signaling pathways.

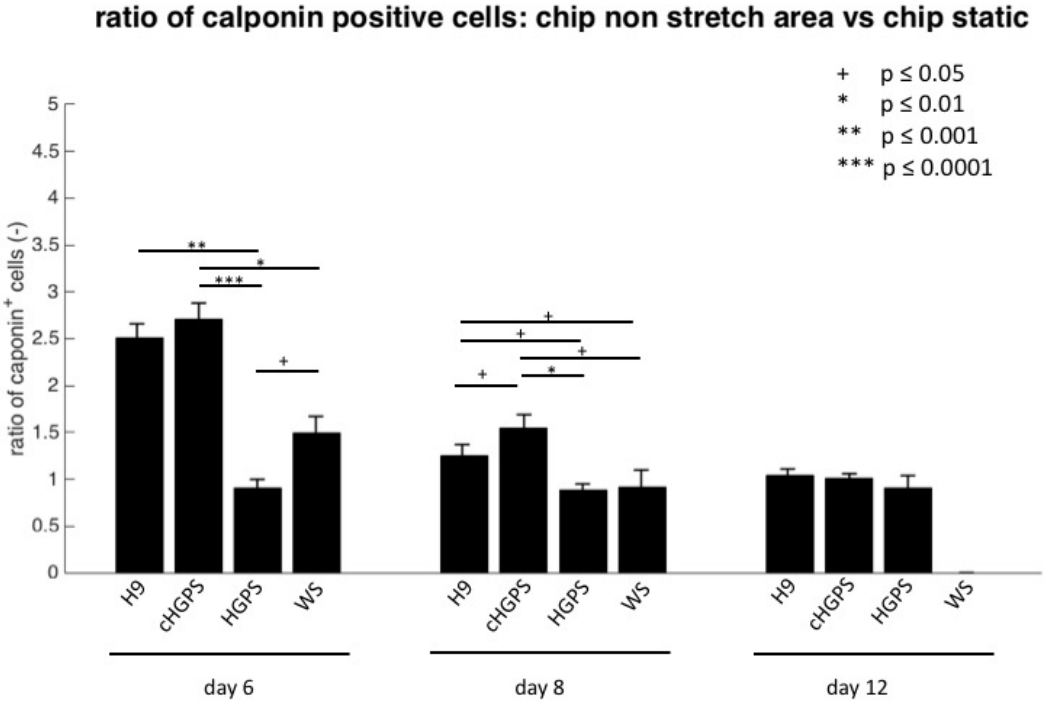

Figure 3.3.12 *Number of calponin positive cells in the non-actively stretched areas normalized respect to the number of calponin positive cells in the static controls. The error bars represent the standard deviation calculated on three samples.*

This finding avails the possibility of performing also high-throughput analysis, such as protein, DNA or RNA extractions, in the microfluidic stretching device, using all the device surface since the signal will be slightly dampened, but still maintain differences with respect to non-stretched cells.

3.2.7. Discussion

Healthy cells lines, namely H9 and cHGPS derived cells, show a rather strong response to external mechanical cues. The results obtained suggest that mechanical strain,

coupled with the appropriate differentiation medium, increases greatly the rate of differentiation but doesn't affect the percentage of differentiated cells upon completion of the differentiation protocol. Probably the mechanical *stimuli* activate a signaling cascade in the cells which in turn drives differentiation, it is not clear however whether the solicited pathways are the same already turned on by the differentiation protocol or if a parallel, and perhaps more stringent, signaling cascade is involved. The increased rate of differentiation discovered also in the non actively stimulated cells advocates in favor of the hypothesis that a major and rather strong signaling pathway is activated, leading, among other things, to an increased intercellular cross-talk and the establishment of a pro-differentiation niche.

Interestingly, similar findings were obtained also analyzing the transcriptome of differentiating smooth muscle cells as reported in § 1.2.2, availing the hypothesis of a response mechanism to mechanical strain common at least to all muscular phenotypes.

It could be interesting to investigate if external mechanical cues alone are able to trigger the differentiation of progenitor cells into mature muscle phenotypes, and if so, if the rate of differentiation in accelerated respect to soluble factors driven differentiation.

On the other hand, the results reported show also an impairment in the response to mechanical strain by senescent cells. In the case of WS cells, there's a mitigated initial response to mechanical cues, but on the longer term the effect appears to be catastrophic leading to generalized cellular death, as demonstrated by the lack of adherent cells by day twelve of mechanical stimulation compared to the normal physiology of the cells cultured in static conditions. In the case of HGPS cells the response to mechanical stretch completely lacks, as the stimulated cells differentiate at the same rate of their static counterparts. This behavior is justified considering the mechanical-coupling between cytoskeleton and heterochromatin role of lamins,

therefore, in the absence of lamin A, the mechanical transduction cascade might be abruptly stopped, hindering beyond repair the ability of the cells to sense and react to mechanical strain.

Despite the models of accelerated aging used in this studies aren't precise reproduction of the complexity of physiological human aging, the fact that both senescent models, though caused by very different biochemical dysregulations, present the inability to correctly react to mechanical stress suggest that the increased vulnerability of the cardiovascular system with age may be caused by pathological mechanotransduction due to the presence of a senescent niche, and further studies may help unravel the complex biomechanical and biochemical mechanism ultimately finding new cures to prevent age aggravated cardiovascular diseases.

4. Final remarks on stretching systems

During this work two different system to provide cyclic mechanical stimulation to cultured cells were developed. The two new technologies established address different experimental requirements mainly due to differences in the biological assays to be performed following the experiment.

The first device, named mesofluidic stretching device, was designed specifically to perform biological analysis that require a high amount of starting material, such as RNA, DNA or protein expression analysis and transcriptome, proteome or sequencing analysis. These assays are widely used in biological experiments: the former to study specific genes activity, as they can give also quantitative results on the relative abundance of proteins or RNA and DNA strands, that imagining analysis isn't able to provide; while the latter are particularly useful as they give an initial broad picture of the biochemical changes elicited by mechanical stimulation, allowing to pinpoint the pathways involved in the mechanotransduction response.

The mesofluidic device has been employed to study the effect of mechanical strain on differentiating muscle cells (myoblasts). These experiments proved the biocompatibility of

the device and more importantly, demonstrated that even a short term exposure to mechanical cues is able to trigger a long lasting and articulated biological response.

The second device developed was aimed at allowing long term stimulation of biological cultures, so it was devised to fit in a standard incubator throughout the mechanical stimulation. In this case the reduced culturing surface and uneven mechanical strain distribution suggest the use of imaging-based biological assays to evaluate the mechanosensitive response of the cultured cells. However, the experiments performed showed that intercellular signaling is able to homogenize the biological response throughout the device surface despite the localized application of mechanical stress, so in these cases also extraction analysis could be performed with minor dampening of the results.

In general, the experiments performed with both the developed devices proved that they are suitable to perform mechanotransduction experiments and they meet the requirements of the assays for which they were designed. The versatility showed by the technologies established, as demonstrated by the experiments performed during this work, opens the way to new studies on cellular mechanotransduction, allowing to better understand how cells sense and respond to mechanical *stimuli* and how the role mechanical forces play in tissue differentiation, development and homeostasis and in pathogenesis.

Chapter four
Conclusion and future perspectives

The external mechanical microenvironment has a tremendous impact on cell behavior, morphology and faith specification and on the development and physiology of tissues and organs. Only in the past decade the scientific community was able to fully grasp the extent of the influence of culturing conditions on biological processes, this appreciation resulted in the need of developing innovative technologies and culturing devices to enable the control of the mechanical *stimuli* imposed to cells in order to mimic the *in vivo* environment and to deepen the knowledge in biological mechanosensing and on the biochemical pathways involved.

In this context the aim of this thesis was to develop novel technologies to allow culturing of cells in mechanically defined conditions. The work was focused mainly on cells typical of the cardiovascular system for two principal reasons: firstly, there's a widespread scientific and clinical interest in the study of this organ-system since cardiovascular diseases are the major cause of death worldwide and cardiovascular toxicity is the principal reason of drug attrition and withdrawal; and secondly, since *in vivo* the cardiovascular system is characterized by very demanding and unique mechanical conditions, it is supposed that mechanotransduction plays an even more relevant role in this context.

The technologies developed and optimized during this work are focused on the establishment of reliable and reproducible pattering techniques, to replicate the *in vivo* cellular polarization and alignment, and on the realization of stretchable culturing devices, to stimulate the cultured cells with physiological or pathological levels of mechanical strain.

Firstly, patterning techniques for rigid substrates creating cell repulsive areas of polyacrylamide hydrogels were developed and optimized. Glass was the choice of rigid substrate since it is optically transparent and its biocompatibility has been already widely demonstrated. In this work two approaches to glass patterning using a cell repulsive polyacrylamide hydrogel were analyzed, eventually it was determined that chemical activated

polymerization of 8% acrylamide and 0.12% bis-acrylamide associated with protection of the supposedly cell adhesive areas through soft-lithography gave the best results in term of pattern resolution and reproducibility. It is now possible to take advantage of this optimized glass pattering technique to thoroughly study the effect of geometrical constrains on cellular behavior and gene expression, and to culture aligned cells to study organized cellular junctions. Specifically in the case of cardiomyocytes, this will allow to investigate in depth the electromechanical coupling of cardiac muscle cells performing ultra resolution microscopy of the intercalated discs to analyze the morphology and patch clamp analysis to evaluate the electrical signal conduction. The results obtained both with healthy cardiomyocytes and with cells carrying mutations on the junction proteins, such as plakophilin whose mutation have been linked to arrhythmogenic right ventricular dysplasia/cardiomyopathy, could then be compared to gather more insight on the relationship between electrical and mechanical signal transduction among cells and, possibly, on the mechanism responsible for the onset of arrhythmias.

Patterning techniques for elastomeric substrates have been expressly realized to be coupled with the developed stretching devices, and thus perform mechanical stimulation of aligned cell cultures.

The stretching devices developed during this work were designed to address specific biological assays commonly used to analyze cellular response.

The first device was intended to be used along with DNA, RNA or protein expression analysis or with full transcriptome or proteome analysis. All this assays require high initial quantity of samples, and in turn give a precise and quantitative read out on the cellular transcriptional activity. To guarantee and adequate number of cells, and thus material to analyze, a fairly large culturing area is required, in this case the culturing area was designed to be $9mm^2$ and for this reason the stretching devices was named mesofluidic stretching devices, as it characteristic dimensions are bigger than those of standard microfluidic technologies. The pattering technique coupled with this device is the physical PDMS pattering, according to

which channels and grooves of specific width are realized on the surface and direct cell topology thanks to the physical constraint due to the different height of the layers. The mechanical stimulation is computer controlled and is applied through ElectroForce® planar biaxial TestBench inserting the device in the machine pincers. The force generated by the machine is much greater than that needed to deform the PDMS device and this allows the use of the physical patterning technique.

The downside of the mesofluidic stretching device is that its size and mechanism of stimulation prevents the possibility of performing the stretching experiment inside an incubator. This inconvenience has been limited realizing an environmental control chamber around the stretching apparatus, but anyways only short term stimulation can be performed. The device was tested studying the effect of mechanical strain on differentiating human myoblasts. This experiments proved that the device is fully biocompatible and that short a term stimulation (30 minutes) in able to trigger a long term biological adaptive response (> 48 hours). Specifically, it was noted that, after a immediate inflammatory response, the stimulated myoblast presented a transcriptional profile similar to that of control cells in later stages of differentiation, suggesting that mechanical strain hastens the differentiation of myoblast into mature myofibers. Currently, we are preforming an experiment with cardiomyocytes seeded at high density and stretched either alongside their main axis or transversally, to evaluate the effect of mechanical stimulation of cellular junctions on the cardiomyocytes gene expression using healthy and diseased models (plakophilin or dystrophin deficient cells).

The second stretching device developed was designed to perform imaging analysis and patch clamp assays. It relays completely on microfluidic technologies and is thus named microfluidic stretching device. In this case the deformation is realized in localized areas through the inflation of a thin PDMS membrane posed on a rectangular-shaped chamber. This kind of assays don’t require large amount of cells so the culturing area in this case was designed to

be 1cm^2, moreover, the deformation in localized only to the inflatable areas, accounting for about 40% of the total surface, so an internal control of non stimulated cells is also provided. The pattering technique developed to be integrated in this device is the chemical PDMS patterning, relying on the same principle of generating polyacrylamide cell repulsive areas perfected for the glass patterning.

The microfluidic stretching device was used to study the effect of mechanical strain on vascular progenitors cells differentiating to vascular smooth muscle cells in collaboration with Prof. Juan Carlos Izpisua Belmonte at the Salk Institute for Biological Studies in La Jolla, CA, USA. These experiments have confirmed the biocompatibility of the device also for long term stimulation, specifically up to twelve days. The immunofluorescence assay marking for calponin, a protein expressed by terminally differentiated vascular smooth muscle cells, has shown a marked effect of mechanical stimulation on differentiation rate, but not on the final percentage of differentiated cells. Interestingly, the same stimulation performed on cellular model of premature aging, namely Hutchinson-Gilford Progeria Syndrome and Werner Syndrome, have shown no or very mitigated biological response to mechanical strain, indicating that in the senescent niche mechanotransduction is somewhat impaired.

Further experiments on differentiating vascular progenitors need to be performed to elucidate the biological mechanism responsible for the impaired mechanosensitive response of the premature aging models, hopefully unravelling the causal link between aging and increased cardiovascular risk.

Moreover, the microfluidic stretching device coupled with the chemical PDMS patterning technique will be used to study the electromechanical coupling of cardiomyocytes, and specifically to investigate the relationship between the electrical signal conduction along aligned cardiomyocytes and stimulation of the cellular junction performing patch clamp analysis on aligned and stretched cardiomyocytes, employing both healthy cells and diseases models such as the aforementioned plakophilin deficient cells, that *in vivo* have been linked with predisposition to arrhythmias.

Given the ability of the microfluidic stretching device to perform long term stretching experiments, it could also be employed to simulate the strain on the cardiovascular system elicited by highly intensive physical activity, such as agonistic motorcycles driving, and analyze the biological response at the cellular level during physical effort and also study how the biological system returns to normal physiology during the rest period.

Overall, this work will allow the study of the mechanosensitive response of the cardiovascular cells and the reproduction of an *in vivo* like environment for the differentiation and maturation of pluripotent stem cells into cells typical of the vasculature, pushing forward our knowledge in the physiological and pathological processes elicited by mechanical *stimuli* and, hopefully, enabling the discovery of novel therapeutic approaches for the prevention and the treatment of cardiovascular diseases.

Bibliography

Chapter one- Introduction

Ascensao A., R. Ferreira, F. Marques, E. Oliveira, V. Azevedo, J. Soares and J. Magalhaes (2007), *Effect of off-road competitive motocross race on plasma oxidative stress and damage markers*, Br J Sports Med, **41** 101-105.

Birukov K. G. (2009), *Cyclic Stretch, Reactive Oxygen Species and Vascular Remodeling*, Antioxidants and Redox Signalling **11** 1651-1667

Bryan M. T., H. Duckles, S. Feng, S. T. Hsiao, H. R. Kim, J. Serbanovic-Canic and P. C. Evans (2014), *Mechanoresponsive Networks Controlling Vascular Inflammation*, Arterioscler. Thromb. Vasc. Biol., **34** 2199-2205

Brown A. E. and D. E. Disher (2009), *Conformational changes and signaling in cell and matrix physics*, Curr. Biol., **19** R781-R789

Collins C. and E. Tzima (2011), *Hemodynamic forces in endothelial dysfunction and vascular aging*, Exp. Gerontol., **46** 185-188

D'Artibale E., A. Tessitore and L. Capranica (2008), *Heart and blood lactate concentration of male road-race motorcyclist,* J. of Sports Sciences, **26:7** 683-689

Dash B. C., Z. Jiang, C. Suh and Y. Qyang (2015), *Induced pluripotent stem cell-derived vascular smooth muscle cells: methods and application*, Biochem. J., **465** 185-194

Furlanello F., A. Bertoldi, M. Dallago, C. Furlanello, F. Fernando, G. Inama, C. Pappone and S. Chierchia (1998), *Cardiac arrest and sudden death in competitive athletes with arrhythmogenic right ventricular dysplasia,* PACE, **21** 331-335

Gerdes A. M. (2002), *Cardiac myocytes remodeling in hypertrophy and progression to failure*, J. Card. Fail., **8** S264-S268

Gimbrone Jr M. A. and G. García-Cardeña (2013), *Vascular endothelium hemodynamics and the pathobiology of atherosclerosis*, Cardiovasc. Pathol., **22** 9-15

Göktepe S., O. J. Abilez, K. K. Parker and E. Khul (2010), *A multiscale model for eccentric and concentric cardiac growth through sarcomerogenesis*, J. Theor. Biol., **265** 433-442

Haga J. H., Y.-S. J. Li and S. Chien (2007), *Molecular basis of the effect of mechanical stretch on vascular smooth muscle cells*, J. Biomech., **40** 947-960

Jaalouk D. E. and J. Lammerding (2009), *Mechanotransduction gone awry*, Nat. Rev. Mol. Cell Biol. **10(1)** 63-73

Karantalis V. and J. M. Hare (2015), *Use of Mesenchymal Stem Cells for Therapy of Cardiac Disease*, Circ. Res., **116** 1413-1430

Knöll R., M. Hoshijima and K. Chien (2003), *Cardiac mechanotransduction and implication for heart diseases*, J. Mol. Med., **81** 750-756

Konttinen T., K. Hakkinen and H. Kyrolainen (2007), *Cardiopulmonary loading in motocross riding*, J of Sports Sciences, **25(9)** 995-999

Kumar V., A. K. Abbas and N. Fausto (2005), *Robbins and Cotran Pathologic Basis of Disease*, Elsevir Sauders, Philadelphia

Mammoto A., T. Mammoto and D. E. Ingber (2012), *Mechanosensitive mechanisms in transcriptional regulation*, J. Cell Sci., **125** 3061-3073

Mihl C., W. R. M. Dassen and H. Kuipers (2008), *Cardiac remodelling: concentric versus eccentric hypertrophy in strenght and endurance athletes*, Netherlands Heart J., **16** 129-133.

Nakayama K. H., L. Hou and N. F. Huang (2014), *Role of Extracellular Matrix Signalling Cues in Modulating Cell Fate Commitment for Cardiovascular Tissue Engineering*, Adv. Healthc. Mater., **3(5)** 628-641

NIH Fact Book (2012) http://www.nhlbi.nih.gov/about/documents/factbook/2012

Nishikawa S., R. A. Goldstein and C. R. Nierras (2008), *The promise of human induced pluripotent stem cells for research and therapy*, Nat. Mol. Cell Bio., **9** 725-729

Peters M. F., S. D. Lamore, L. Guo, C. W. Scott and K. L. Kolaja (2015) *Human Stem Cell-Derived Cardiomyocytes in Cellular Impendance Assays: Bringing Cardiotoxicity Screening to the Front Line*, Cardiovasc. Toxicol., **15** 127:139

Shao Y., J. Sang and J. Fu (2015), *On human pluripotent stem cell control: the rise of 3D bioengineering and mechanobiology*, Biomaterials, **52** 26-43

Stewart M. P., J. Helenius, Y. Toyoda, S. P. Ramanathan, D. J. Muller and A. A. Hyman (2011), *Hydrostatic pressure and the actomyosin cortex drive mitotic cell rounding*, Nature, **469** 226-230

Takahashi K. And S. Yamanaka (2006), *Induction of Pluripotent Stem Cells from Mouse Embryonic and Adult Fibroblast Cultures by Defined Factors*, Cell,**126** 651-655

Takahashi K., Y. Kakimoto, K. Toda and K. Naruse (2013), *Mechanobiology in cardiac physiology and diseases*, J. Cell. Mol. Med., **17** 225-232.

Takahashi K., K. Tanabe, M. Ohnuki, M. Narita, T. Ichisaka, K. Tomoda and S. Yamanaka (2007), *Induction of Pluripotent Stem Cells from Adult Human Fibroblasts by Defined Factors*, Cell, **131** 861-872

Tarbell J. M., Z.-D. Shl, J. Dunn and H. Jo (2014) *Fluid Mechanics, Arterial Diseases, and Gene expression*, Ann. Rev. Fluid. Mech. **46** 591-614

WHO (2012) http://www.who.int/mediacentre/factsheets/fs310/en/

Xin M., E. N. Olson and R. Bassel-Duby (2013), *Mending broken hearts: cardiac development as a basis for adult heart regeneration and repair*, Nat. Rev. Mol. Cell Bio., **14** 529-541

Yang Y.-C., X.-D. Wang, K. Huang, L. Wang, Z.-L. Jiang and Y.-X. Qui (2014), *Temporal phosphoproeomics to investigate the mechanotransduction of vascular smooth muscle cells in response to cyclic stretch*, J. Biomech., **47** 3622-3629

Chapter two- Patterning techniques

Aragona M., T. Panciera, M. Manfrin, S. Giulitti, F. Michielin, N. Elvassore, S. Dupont and S. Piccolo (2013), *A mechanical checkpoint controls multicellular growth through YAP/TAZ regulation by actin-processing factors,* Cell **154** 1047-1059

Dupont S., L. Morsut, M. Aragona, E. Enzo, S. Giulitti, M. Cordenonsi, F. Zanconato, J. Le Digabel, M. Forcato, S. Bicciato, N. Elvassore and S. Piccolo (2011), *Role of YAP/TAZ in mechanotransduction*, Nature **474** 179-183

Martewicz S. (2015) *Human Pluripotent Stem Cell-based microtechnologies for in vitro modeling of cardiac diseases*, Phd Thesis, Scuola di dottorato di ricerca in bioscienze e biotecnologie, Università degli Studi di Padova

Mc Cain M. L. and K. K. Parker (2011), *Mechanotransduction: the role of mechanical stress, myocyte shape and cytoskeletal architecture on cardiac function*, Pflugers Arch.-Eur. J. Physiol., **462** 89-104

Pelham J.R. and Y-L Wang (1997), *Cell locomotion and focal adhesions are regulated by substrate flexibility*, Proc. Natl. Acad. Science **94** 13661-13665

Perl A., D. N. Reinhoudt and J. Huskens (2009), *Microcontact Printing: Limitations and Achievements*, Adv. Mater., **21** 2257-2268

Simmons C. S., A. J. S. Ribeiro and B. L. Pruitt (2013), *Formation of composite polyacrylamide and silicone substrates for independent control of stiffness and strain*, Lab Chip, **13(4)** 646-649

Tse R. J. and A. J. Engler (2010), *Preparation of hydrogel substrates with tunable mechanical properties*, Curr. Protoc. Cell Biol. **47** 10.16.1-10.16.16

Wang H-B., M. Dembo and Y-L Wang (2000), *Substrate flexibility regulates growth and apoptosis of normal but not transformed cells*, Am J Physiol Cell Physiol. **279** C1345-C1350

Chapter three- Stretching devices

Amit M., C. Shariki, V. Margulets and J. Itskovitz-Eldor (2004), *Feeder Layer- and Serum-Free Culture of Human Embryonic Stem Cells*, Biol. Reprod. **70** 837-845.

Chen Q., W. Li, Z. Quan and B. E. Sumpio (2003), *Modulation of vascular smooth muscle cell alignment by cyclic strain is dependent on reactive oxygen species and P38 mitogen-activated protein kinase*, J. Vasc. Surg. **37** 660-668

Cheung H.-H, D. Pei and W.-Y. Chan (2015), *Stem cell aging in adult progeria*, Cell Regeneration 4:6

Dahl K. N., P. Scaffidi, M. F. Islam, A. G. Yodh, K. L. Wilson and T. Misteli (2006), *Distinct structural and mechanical properties of the nuclear lamina in Htchinson-Gilford progeria syndrome*, PNAS **103** 10271-10276

Dan P., E. Velot, V. Decot and P. Menu (2015), *The role of mechanical stimuli in the vascular differentiation of mesenchymal stem cells*, J. Cell Sci. **128** 2415-2422

El-Mezgueldi M. (1996), *Calponin*, Int. J. Biochem. Cell. Biol **28** 1185-1189

Huang N. F. and S. Li (2008), *Mesenchymal stem cells for vascular regeneration*, Regen. Med. **3** 877-892.

Kurian L., I. Sancho-Martinez, E. Nivet, A. Aguirre, K. Moon, C. Pendaries, C. Volle-Challier, F. Bono, J.-M. Herbert, J. Pulecio, Y. Xia, M. Li, N. Montserrat, S. Ruiz, I. Dubova, C. Rodriguez, A. M. Denli, F. S. Boscolo, R. D. Thiagarajan, F. H. Gage, J. F. Loring, L. C. Laurent and J. C. Izpisua Belmonte (2013), *Conversion of human fibroblasts to agioblasts-like progenitor cells*, N. Meth. **10** 77-83

Li S., J. Lao, B. P. Chen, Y. S. Zhao, J. Chu, K. D. Chen, T. C. Tsou, K. Peck and S. Chien (2003) *Genomic analysis of smooth muscle cells in 3-dimensional collagen matrix* FASEB J. **17** 97-99

Liu G.-H. B. Z. Barkho, S. Ruiz, D. Diep, J. Qu, S.-L. Yang, A. D. Panopoulos, K. Suzuki, L. Kurian, C. Walsh, J. Thomposn, S. Boue, H. L. Fung, I. Sancho-Martinez, K. Zhang, J. Yates III and J. C. Izpisua Belmonte (2011a), *Recapitulation of premature ageing with iPSCs from Hutchinson-Gilford progeria syndrome*, Nature **472** 221-225

Liu G.-H., K. Suzuki, J. Qu, I. Sancho-Martinez, F. Yi, M. Li, S. Kumar, E. Nivet, J. Kim, R. D. Soligalla, I. Dubova, A. Goebl, N. Plongthongkum, H.-L. Fung, K. Zhang, J. F. Loring, L. C. Laurent and J. C. Izpisua Belmonte (2011b), *Targeted Gene Correction of Laminopathy-Associated LMNA Mutations in Patient-Specific iPSCs*, Cell Stem Cell **8** 688-694

Michelin F. (2009), *Sviluppo di una piattaforma microfluidica per il controllo della concentrazione di ossigeno in culture cellulari*, M.Sc. in Ingegneria Chimica e dei Processi Industriali, Università degli studi di Padova.

Michielin F., E. Serena, P. Pavan and N. Elvassore (2015) *Microfluidic-assisted cyclic mechanical stimulation affects cellular membrane integrity in a human muscular dystrophy in vitro model*, RSC adv. **5** 98429-98439

Pichierri P., F. Ammazzalorso, M. Bignami and A. Franchitto (2011), *The Werner syndrome protein: linking the replication checkpoint response to genome stability*, Aging **3(3)** 311-318

Pollex R. L. and R. A. Hegele (2004), *Hutchinson-Gilford progeria syndrome*, Clin. Genet. **66** 375-381

Salameh A., A. Wustmann, S. Karl, K. Blanke, D. Apel, D. Rojas-Gomez, H. Franke, F. W. Mohr, J. Janousek and S. Dhein (2010), *Cuclic Mechanical Stretch Induces Cardiomocyte Orientation and Polarization of the Gap Junction Protein Connexin43*, Circ. Res. **106** 1592-1602

Scaffidi P. and T. Misteli (2006), *Lamin A-Dependent Nuclear Defects in Human Aging*, **312(5776)** 1059-1063

Schmelter M., B. Ateghang, S. Helming, M. Wartenberg and H. Sauer (2006) *Embryonic stem cells utilize reactive oxygen species as transducers of mechanical strain-induced cardiovascular differentiation*, FASEB J. **20** E294-E306

Shimamoto A., K. Yokote and H. Tahara (2015), *Werner Syndrome-specific induced pluripotent stem cells: recovery of telomere function b reprogramming*, Front. Genet. **6** 1-13

Standley P.R., A. Cammarata, B. P. Nolan, C. T. Purgason, M. A. Stanley and A. Camaratta (2002) *Cyclic stretch induces vascular smooth muscle cell alignment via NO signaling*, Am. J. Physiol-Heart C **283** H1907-H1914

Tarbell J. M., Z.-D. Shl, J. Dunn and H. Jo (2014) *Fluid Mechanics, Arterial Diseases, and Gene expression*, Ann. Rev. Fluid. Mech. **46** 591-614

Verstraeten V. L. R. M., J. Y. Ji, K. S. Cummings, R. T. Lee and J. Lammerding (2008), *Increased mechanosensitivity and nuclear stiffness in Hutchinson-Gilford progeria cells: effects of farnesyltransferase inhibitors,* Aging Cell 383-393

Zhang W., J. Li, K. Suzuki, J. Qu, P. Wang, J. Zhou, X. Liu, R. Ren, X. Xu, A. Ocampo, T. Yaun, J. Yang, Y. Li, L. Shi, D. Guan, H. Pan, S. Duan, Z. Ding, M. Li, F. Yi, R. Bai, Y. Wang, C. Chen, F. Yang, X. Li, Z. Wang, E. Aizawa, A. Goebl, R. D. Soligalla, P. Reddy, G.-H. Liu and J.C Izpisua Belmonte (2015), *A Werner Syndrome stem cell model unveils heterochromatin alterations as a driver of human aging*, Aging Stem Cells **348** 1160-1163